Efficient Estimation of DSGE Models with Nonlinearities and State Dependence

Eva F. Janssens[†] and Sean McCrary[‡]

March, 2025

Most Recent Version

Abstract

This paper introduces a computationally efficient and accurate method for estimating nonlinear DSGE models, leveraging advances in local linear solution methods combined with the time-varying Kalman filter – the optimal linear filter given the solution method. We show that this approach is theoretically equivalent to using the true global nonlinear model solution with the Extended Kalman Filter but at a fraction of the computational cost. Applying the filter to the Diamond-Mortensen-Pissarides (DMP) and standard New Keynesian (NK) models, we confirm its accuracy, and find evidence for state-dependence that is absent in a linear solution of the model. Combining both model frameworks into an NKDMP model, we find that variations in job creation profitability (flow surplus) induce state dependence in monetary policy transmission, yielding time-varying impulse responses and Phillips Multipliers that fluctuate with the business cycle. We support this finding with reduced-form model-free empirical evidence. In our estimated quantitative model, the Phillips Multiplier is twice as small after recessions as after expansions.

Keywords: numerical methods, Taylor projection, labor search, full-information estimation

JEL classification codes: C63, C68, C32, E32, E52, J64

* Acknowledgements: We are grateful for Hilde Bjornland's discussion at Midwest Econometrics' mentoring meeting, and for the helpful comments of Ryan Michaels, Francesco Furlanetto, Rüdiger Bachmann, Yoosoon Chang, seminar attendants at UNC, and conference participants at SEA, IAAE, Midwest Macro, Midwest Econometrics, and T2M. This paper was earlier presented under the name "Unemployment and the State-Dependent Effects of Monetary Policy". Any errors are our own.

Contact information:
† Eva F. Janssens: University of Michigan, Department of Economics. Email: evafj@umich.edu
‡ Sean McCrary: Ohio State University, Department of Economics. E-mail: mccrary.65@osu.edu

1 Introduction

Nonlinearities play a fundamental role in macroeconomic dynamics, and recent empirical evidence underscores their importance. For instance, studies suggest that the Phillips curve is nonlinear or may have a slope that changes over time (Benigno and Eggertsson, 2024; Hazell, Herreno, Nakamura, and Steinsson, 2022; Stock and Watson, 2020, and others) and a growing literature finds that the impact and transmission of economic shocks depend on both the state of the economy and the magnitude and direction of the shock (e.g., Eichenbaum, Rebelo, and Wong, 2022; Tenreyro and Thwaites, 2016). While macroeconomic models inherently feature such nonlinearities, whether these features affect model predictions crucially depends on the choice of solution and estimation method. The frontier approach to full-information estimation of nonlinear Dynamic Stochastic General Equilibrium (DSGE) models – nonlinear model solutions and nonlinear filters (Fernández-Villaverde and Rubio-Ramírez, 2007; Winschel and Krätzig, 2010) – is computationally costly. As a result, researchers frequently resort to computationally simpler alternatives retaining linearity,[1] despite broad recognition that linear methods can yield substantially different parameter estimates.[2]

This paper proposes a computationally efficient full-information estimation method for nonlinear DSGE models, leveraging recent advances in the macroeconomic computational literature. Particularly, we build on the solution approaches of Fernández-Villaverde and Levintal (2018); Levintal (2018) and Mennuni, Rubio-Ramírez, and Stepanchuk (2024), and show that models solved using local linear approximation methods can be mapped into a time-varying linear state space model, for which the likelihood can be evaluated using the time-varying Kalman filter, which is not only fast, but, conditional on the solution method, optimal. In addition, we show that this combination of solution method and filter is equivalent to using the true global model solution combined with the Extended Kalman filter – a standard nonlinear filter. Note, however, that a global model solution is many times more costly to compute than a local linear model solution, and hence, this equivalence implies large computational savings. While the accuracy of this estimation procedure depends on the precision of the local linear approximations, economic state

[1] For example, estimating a linearized version of the model and applying those parameters to a nonlinear solution (Aruoba, Cuba-Borda, and Schorfheide, 2018), or using moment-based estimation methods around two different steady states (Eichenbaum, Puglisi, Rebelo, and Trabandt, 2025).

[2] See, for example, Fernández-Villaverde and Rubio-Ramírez (2005), An and Schorfheide (2007), Amisano and Tristani (2010), and Gust, Herbst, López-Salido, and Smith (2017) and Judd, Maliar, and Maliar (2017) pointing out that perturbation methods make unacceptably large approximation errors relative to the true global solution.

variables generally exhibit limited period-to-period variation, implying that the method is highly accurate in practice.

Local linear solution methods can be applied to a large class of models, and allow a researcher to capture important nonlinearities of their model in a computationally efficient way. This includes allowing for state-dependence, where propagation can vary at each point of the state space, and moving away from certainty equivalence, in a way where, in contrast to a second-order perturbation around the steady state (Schmitt-Grohé and Uribe, 2004), risk affects elasticities. Our simulations show that Levintal (2018)'s local linear solution method is comparable in accuracy to a global model solution for the Diamond-Mortensen-Pissarides (DMP) model,[3] which is a model with labor search frictions known to be highly nonlinear and poorly approximated by perturbation methods (Petrosky-Nadeau and Zhang, 2017). A Monte Carlo that simulates data from this model solved using a global solution method and benchmarks our proposed filtering algorithm against a global solution method with a particle filter, and the Extended Kalman filter (EKF), shows, consistent with our theory, our method to be equivalent to the EKF, and, in finite samples, more accurate than the particle filter.

Next, we apply our estimation procedure to the canonical three-equation New Keynesian (NK) model (see, e.g., Gali, 2015; Herbst and Schorfheide, 2016), which is central to modern monetary policy analysis. We demonstrate that our nonlinear estimation method can obtain 100,000 draws of the posterior in a little over nine minutes – less than twice the time required to estimate a linear version in Dynare[4] – in stark contrast to the particle filter as reviewed in An and Schorfheide (2007), where nonlinear estimation of the model solved with second-order perturbation is reported to be about 200 times slower than linear estimation. Even in this simple model, accounting for nonlinearities enhances the model fit. Importantly, the estimated nonlinear model yields insights into the variation of the effects of monetary policy and discount factor shocks over time. Specifically, we find that in the early 1980s, the initial impact of these shocks on output and employment was considerably larger than in the mid-2000s. This finding is consistent with the mild flattening of the Phillips curve between the 1980s and 2000s, documented empirically by Stock and Watson (2020) and Hazell et al. (2022).

As the main application of this paper, we use our newly proposed methodology to further study state-dependence in monetary policy transmission. In particular, we provide model-

[3] Diamond (1982), Mortensen (1982), and Pissarides (1985)

[4] Adjemian et al. (2024).

free reduced-form empirical evidence that monetary policy shocks have larger and more persistent real-side effects during times when the profitability of job creation (flow surplus) is low. This result is robust to using three proxies for surplus, three monetary policy instruments, and two econometric methodologies. This empirical evidence motivates a New Keynesian model with DMP-style labor market frictions, which we solve and estimate nonlinearly.

Our methodological framework allows filtering the evolution of underlying economic states over time and assessment of their impact on shock propagation, a valuable tool for policymakers. The results reveal substantial variation in impulse response functions, with periods where shocks have either minimal or large effects on the economy. A key metric for policymakers is the cost of monetary policy, captured by the inflation-unemployment trade-off, commonly known as the Phillips Multiplier – which can be loosely interpreted as the slope of the Phillips curve. The model and filtering framework enable the computation of the Phillips Multiplier dynamically at each point in time, and confirms a countercyclical pattern. Specifically, in low-surplus periods (i.e, following recessions), the Phillips curve flattens, with the Phillips Multiplier close to zero (around -0.03 or -0.02). In high-surplus periods (i.e., following expansions), the Phillips curve steepens, and the Multiplier can double, reaching values as large as -0.07 – estimates well in line with existing studies such as Barnichon and Mesters (2021) and Hazell et al. (2022). This range of time-variation in the Phillips Multiplier aligns with the empirical findings of Gitti (2024) on differences in the slope of the Phillips curve.

Both our reassessment of the three-equation New Keynesian model and our estimated NKDMP model indicate that several nonlinearities previously examined in the literature – such as the flattening of the Phillips curve (Hazell et al., 2022), state-dependence in monetary policy transmission across the business cycle (Tenreyro and Thwaites, 2016), and the cyclicality of the Phillips multiplier in relation to market tightness (Benigno and Eggertsson, 2024; Gitti, 2024) – may not necessarily require the introduction of additional frictions, nonlinearities, kinks or time-varying parameters. Instead, these nonlinearities are inherently present in standard macroeconomic models but become evident only when employing nonlinear solution and estimation methods.

Related literature Our contribution to filtering and estimation is a novel framework for nonlinear DSGE models. We show that models solved using local linear approximation methods, such as Levintal (2018) and Mennuni et al. (2024), can be mapped into time-varying linear state-space models and filtered using the time-varying Kalman filter,

enabling fast and accurate estimation of nonlinear models. This relates to a broader literature on nonlinear DSGE estimation. A key benchmark is Fernández-Villaverde and Rubio-Ramírez (2007), who introduce the particle filter to economics. Particle filtering suffers from high computational costs due to the curse of dimensionality, evident in Gust et al. (2017) who estimate a globally solved model using the particle filter, needing many particles and parallel computing with many nodes. Similarly, Farmer (2021) proposes a discretization filter for second-order perturbations, but discretizing the state space is computationally intensive and also suffers from the curse of dimensionality. Winschel and Krätzig (2010) aim to resolve this curse of dimensionality by using sparse grid methods and parallelization, but such methods remain computationally costly. In contrast, our proposed method is accurate as well as computationally efficient and feasible on a standard desktop computer without relying on parallelization. Other approaches, such as Aruoba et al. (2018) and Harding, Lindé, and Trabandt (2022), estimate a linearized DSGE model and evaluate its policy implications using a nonlinear model solution. While computationally attractive, this method may be biased when the local perturbation deviates significantly from the global solution – a key issue in our applications given the well-documented nonlinearities in labor search models (see, e.g., Petrosky-Nadeau and Zhang, 2017).

Our quantitative model builds on a long tradition of New Keynesian models and search-and-matching models à la Diamond (1982), Mortensen (1982), and Pissarides (1985), and more recent work integrating both frameworks, such as Christiano, Eichenbaum, and Trabandt (2016) and Thomas (2011), with key contributions from Galí, Smets, and Wouters (2012), Blanchard and Galí (2010), Krause and Lubik (2007), and Gertler, Sala, and Trigari (2008). The model is most similar to Krause, Lopez-Salido, and Lubik (2008) but differs in a key respect: whereas they use log-linearization, which fixes flow profit at its steady-state value, we employ a nonlinear solution that allows flow profit to evolve over time. This enables us to show that monetary transmission varies with labor market conditions, establishing state dependence as a key feature of New Keynesian models with search frictions – our primary contribution relative to this literature.

At last, our paper relates to a long literature studying the Phillips (1958) curve, including its nonlinearities and time variation in its slope, as examined in Coibion and Gorodnichenko (2015), Smith, Timmermann, and Wright (2023), and others. Both Smith et al. (2023) (empirically) and Benigno and Eggertsson (2023) (model and empirics) argue that the Phillips curve is steeper in tighter labor markets, a finding consistent with our empirical and model-based results. Benigno and Eggertsson (2023) model this within a New

Keynesian framework by introducing a kink in wage setting around a market tightness of one, which mechanically induces a kink in the Phillips curve. We differ from this approach by showing that state dependence does not need to be explicitly modeled in a New Keynesian model; rather, it emerges endogenously from its nonlinear solution. A different but related literature suggests that nonlinearities and state dependence may arise from pricing setting frictions rather than labor market frictions, with contributions from Dotsey, King, and Wolman (1999), Gertler and Leahy (2008), and more recently, Harding et al. (2022) and Harding, Lindé, and Trabandt (2023). Instead, our focus is on labor market frictions as the primary source of state dependence. Finally, a recent study by Lahcen, Baughman, Rabinovich, and van Buggenum (2022) builds on the money search tradition of Berentsen, Menzio, and Wright (2011), showing that small-surplus calibrations imply state-dependent inflation costs. We view the money search literature as complementary, as it abstracts from the nominal rigidities central to New Keynesian frameworks and, consequently, from the role of active monetary policy, which is our primary focus in this application.

Outline The rest of this paper is structured as follows. Section 2 presents our methodological contribution. Section 3 demonstrates the performance of this method using simulations of the Diamond-Mortensen-Pissarides model. Section 4 presents the reassessment of the three-equation New Keynesian model. Section 5 presents the model of our main application, and Section 6 presents reduced-form evidence supporting our main channel of state-dependence. Section 7 presents our quantitative model results, and Section 8 concludes.

2 Local Linear Approximations and Time-Varying Kalman Filtering

In this section, we present our main methodological contribution: a full-information estimation method for DSGE models solved using local linear approximation methods. We center our discussion on our preferred computational algorithm, Taylor projections (Fernández-Villaverde and Levintal, 2018; Levintal, 2018), as we find it to be computationally more efficient than alternative methods. However, the filtering approach outlined below is more general and can be applied to other local linearization techniques, such as Dynamic Perturbation, as in Mennuni et al. (2024).

2.1 Local Linear Approximation Methods

A standard Dynamic Stochastic General Equilibrium (DSGE) model can be represented as follows (Schmitt-Grohé and Uribe, 2004):

$$\mathbb{E}_t \left[f(x_{t+1}, x_t, z_{t+1}, z_t, \eta_{t+1}) \right] = 0, \tag{1}$$

where x_t represents the control variables, and the state variables z_t can be partitioned into endogenous variables $z_{1,t}$ and exogenous variables $z_{2,t}$. Exogenous variables are assumed to follow a stationary VAR(1): $z_{2,t+1} = Az_{2,t} + B\eta_{t+1}$, where η_t is a vector of Gaussian exogenous shocks. Endogenous variables $z_{1,t+1}$ depend on z_t through an unknown nonlinear mapping. Hence, a solution to (1) is characterized by two implicit functions,

$$z_{t+1} = h(z_t)$$

and the policy function:

$$x_t = g(z_t).$$

A and B are assumed to be known functions of structural parameters (that may have to be estimated), while g and h are the unknown functions that we wish to solve for.

Taylor Projection (Levintal, 2018) The Taylor projection method consists of four main steps. In this exposition and in our filtering method, we focus on the first-order Taylor projection.

In the first step, the policy function $g(x_t)$ and law of motion $h(x_t)$ are approximated using linear functions:

$$\tilde{g}(z_t; \Theta) = \Theta_1 + \Theta_2 z_t \tag{2}$$

$$\tilde{h}(z_t; \Theta) = \Theta_3 + \Theta_4 z_t \tag{3}$$

In step two, the residual function $R(z_t, \Theta)$ is constructed by substituting $x = \tilde{g}(z_t; \Theta)$ and $z_{t+1} = \tilde{h}(z_t; \Theta)$ into the equilibrium condition (1):

$$R(z_t, \Theta) = \mathbb{E}_t \left[f(\tilde{g}(\tilde{h}(z_t)), \tilde{g}(z_t), \tilde{h}(z_t), z_t, \eta_{t+1}) \right] \approx 0. \tag{4}$$

The objective is to find Θ such that the residual function is equal to zero.

To do so, in step three, the residual function is approximated using a Taylor series expansion around a specific point z_0, retaining terms up to first order:

$$R(z_t, \Theta) \approx R(z_0, \Theta) + \left.\frac{\partial R(z, \Theta)}{\partial z}\right|_{z=z_0} (z - z_0). \tag{5}$$

At last, in step four, one solves for the optimal Θ^* such that the Taylor series satisfies:

$$\begin{aligned} R(z_0, \Theta) &= 0 \\ \frac{\partial}{\partial x} R(z, \Theta)\Big|_{z=z_0} &= 0. \end{aligned}$$

Since z may consist of multiple state variables, our notation for the first-order derivatives intends to capture all partial derivatives. Solving this system gives a set of state-dependent parameters $\Theta^* = \Theta(z_0)$, yielding an approximate solution $\tilde{g}(z, \Theta^*)$ and $\tilde{h}(z, \Theta^*)$ around z_0. In our examples that follow, we will make more explicit how these steps work.

Dynamic Taylor Projection Instead of computing a Taylor Projection at a single point z_0, one can compute a Taylor Projection at each point along a simulation path, similar in spirit to the Dynamic Perturbation method in Mennuni et al. (2024). This yields highly accurate results, as we will show in our examples. Given that each solution $\tilde{g}(z, \Theta^*)$ and $\tilde{h}(z, \Theta^*)$ is accurate locally around z_0, as long as variables do not change too much from one time period z_t to the next z_{t+1}, the mistakes made by the dynamic implementation of the solution method will be small. Since economic systems, e.g., business cycles, tend to be relatively slow-moving, this is typically the case.

Solving the nonlinear system to recover policy coefficients involves handling expectation operators. Prior studies approximate expectations using monomial integration. We show in the Appendix that, in our applications, assuming local policies are linear in logs, expectations can be solved analytically, yielding an exact nonlinear system. This approach has two advantages: (i) it eliminates errors from integral approximations and (ii) accelerates residual evaluation while providing exact Jacobian terms, speeding up Newton iterations. While not essential, models designed for log-linearization may share this feature, making exact expectation solutions a practical advantage.

2.2 Time-Varying Kalman Filter

Consider a standard linear state space model:

$$y_t = Z s_t + d + \varepsilon_t \tag{6}$$

$$s_{t+1} = T s_t + c + R\eta_t \tag{7}$$

with ε_t i.i.d. measurement error with variance-covariance matrix H, and η_t i.i.d. with variance-covariance Q. y_t is the set of observed variables, s_t are the states, which are assumed unobserved.

It is well-known that linearized DSGE models can be mapped into a linear state space form, and hence, its parameters can be estimated using standard Kalman filtering approaches. For a textbook treatment, consider Herbst and Schorfheide (2016). For a model that is log-linearized around the steady state, the matrices Z, d, H, Q, T, c and R depend on structural model parameters, but are constant and do not vary over time.

Our contribution is the insight that when a model is solved using a local linear approximation method such as Levintal (2018)'s Taylor Projection method outlined above, the local linear model solution can be mapped into a *time-varying* state space model, and the model's states can be filtered using a time-varying Kalman Filter, which, in that case, is the optimal linear filter.

To map things back into previous notation, note that the unobserved states s_t of the state-space model will be functions of model state variables z_t. Assume the Taylor Projection method around a specific point z is used to obtain an approximation $x_t = \Theta_1^z + \Theta_2^z z_t$ and $z_{t+1} = \Theta_3^z + \Theta_4^z z_t$, where the superscript z indicates that these are the solution matrices based on the Taylor projection around z. Given that our model solution is now fully characterized by linear equations, we can map the model solution into a linear state space form:

$$y_t = Z_z s_t + d_z + \varepsilon_t \tag{8}$$

$$x_{t+1} = T_z s_t + c_z + R\eta_t \tag{9}$$

where Z_z, T_z, d_z and c_z contain elements of the matrices Θ_1^z, Θ_2^z, Θ_3^z, Θ_4^z of the local approximation of the model solution. Variance-covariance matrices H and Q, as well as shock selection matrix R typically do not have state-dependence when using this solution

Algorithm 1 Time-Varying Kalman Filtering with Taylor Projections

Initialize: Set $t = 0$, start s_0 in the steady state, and initialize covariance $P_{0|0}$.
while $t \leq T$ **do**
Taylor Projection Step:
Solve the model using Taylor Projections at $\hat{s}_{t|t-1}$, obtaining the time-varying system:

$$y_t = Z_{\hat{s}_{t|t-1}} s_t + d_{\hat{s}_{t|t-1}} + \varepsilon_t, \quad \varepsilon_t \sim \mathcal{N}(0, H) \tag{10}$$

$$x_{t+1} = T_{\hat{s}_{t|t-1}} s_t + c_{\hat{s}_{t|t-1}} + R\eta_t, \quad \eta_t \sim \mathcal{N}(0, Q) \tag{11}$$

Update Step:
Compute the Kalman gain:

$$K_t = P_{t|t-1} Z'_{\hat{s}_{t|t-1}} \left(Z_{\hat{s}_{t|t-1}} P_{t|t-1} Z'_{\hat{s}_{t|t-1}} + H \right)^{-1} \tag{12}$$

Update the state estimate using the new observation y_t:

$$\hat{s}_{t|t} = \hat{s}_{t|t-1} + K_t \left(y_t - Z_{\hat{s}_{t|t-1}} \hat{s}_{t|t-1} - d_{\hat{s}_{t|t-1}} \right) \tag{13}$$

Update the covariance:

$$P_{t|t} = (I - K_t Z_{\hat{s}_{t|t-1}}) P_{t|t-1} \tag{14}$$

Prediction step:
Compute the predicted state estimate:

$$\hat{s}_{t+1|t} = T_{\hat{s}_{t|t-1}} \hat{s}_{t|t} + c_{s_{t|t-1}} \tag{15}$$

Compute the predicted covariance:

$$P_{t+1|t} = T_{\hat{s}_{t|t-1}} P_{t|t} T'_{\hat{s}_{t|t-1}} + RQR' \tag{16}$$

Advance time: Set $t \leftarrow t + 1$ and repeat.
end while

method, so these matrices do not need subscripts z. Innovation matrix η_t corresponds exactly to η_t in our general notation for the DSGE model above.

The Kalman filter is valid and optimal, even when the system matrices Z, d, T and c are time-varying, as long as this time-dependence is fully known when conditioning on the information set $\mathcal{Y}_{t-1} = \{y_{t-1}, y_{t-2}, ...\}$. This follows from the recursive definition of the Kalman filter.[5] This allows us to replace the subscript z in Equations (8)-(9) by $\hat{s}_{t|t-1}$, our

[5]This is a well-established result; see, for example, Durbin and Koopman (2012) and Hamilton (1994).

prediction for the state s_t using all information up to and including time $t-1$, and implies the filtering procedure outlined in Algorithm 1.

In words, what Algorithm 1 does is it computes a local linear approximation of the policy functions g and law of motion h at the best prediction for the current state s_t, denoted $\hat{s}_{t|t-1}$ (which implies a prediction for x_t) based on all past data up to and including $t-1$. We can map this linear approximate model solution into the linear state space form of Equations (8)-(9), and use the Kalman filter to obtain a prediction for the next state, $\hat{s}_{t+1|t}$. We then repeat the procedure, by computing a local linear model solution around $\hat{s}_{t+1|t}$, mapping this model solution into state space form, and obtaining a new prediction $\hat{s}_{t+2|t+1}$, etc.

2.3 Relation to the Extended Kalman Filter

To those familiar with nonlinear filtering, the filtering algorithm above may sound related to the Extended Kalman Filter (EKF), as both involve local linearization of a nonlinear system. For those unfamiliar, consider the following nonlinear (potentially time-varying) state space model:

$$y_t = Z(s_t) + \varepsilon_t \tag{17}$$

$$s_{t+1} = T(s_t) + R\eta_t \tag{18}$$

where ε_t and η_t have variance-covariance matrix H and Q.[6] Following notation in Durbin and Koopman (2012), define

$$\dot{Z}_t = \left.\frac{\partial Z(s_t)}{\partial s_t'}\right|_{s_t=\hat{s}_{t|t-1}}, \quad \text{and} \quad \dot{T}_t = \left.\frac{\partial T(s_t)}{\partial s_t'}\right|_{s_t=\hat{s}_{t|t}}$$

Instead of filtering the nonlinear system (17)-(18), the EKF applies the Kalman filter on the linearized system:

$$y_t = \dot{Z}_t s_t + d_t + \varepsilon_t, \quad d_t = Z(\hat{s}_{t|t-1}) - \dot{Z}_t \hat{s}_{t|t-1}, \quad \varepsilon_t \sim (0, H)$$
$$s_{t+1} = \dot{T}_t s_t + c_t + R\eta_t, \quad c_t = T(\hat{s}_{t|t}) - \dot{T}_t s_{t|t}, \quad \eta_t \sim (0, Q)$$

EKF when the global model solution is known First, assume that the solutions to the equilibrium conditions in Equation (1), given by functions $x_t = g(z_t)$ and $z_{t+1} = h(z_t)$, exist

[6] The EKF also allows for time-varying volatility that potentially depends on state s_t, but for the arguments in this section, we omit these intricacies.

and are known. These functions map into the nonlinear state space form (17)-(18) through the nonlinear functions $Z(s_t)$ and $T(s_t)$. It follows that in EKF, the first-order Taylor expansion of the nonlinear functions $Z(\cdot)$ and $T(\cdot)$ involves a first-order Taylor expansion of the nonlinear model solution $x_t = g(z_t)$ and $z_{t+1} = h(z_t)$. Hence, the distinction between the EKF applied to the global model solution and the time-varying Kalman filter applied to the Taylor Projection solution lies in at what point in the algorithm the linearization is applied.

In the Taylor Projection method, the residual function is approximated using a first-order Taylor series expansion around a specific point z. In our algorithm, we expand around $\hat{z}_{t|t-1}$, that is, the MSE-optimal prediction for z given our information up to $t-1$. Note that the policy function $g(z)$ and law of motion $h(z)$ are defined *implicitly* through the residual function defined by the equilibrium condition in Equation (1), given by

$$R(z_t, \Theta) = \mathbb{E}_t \left[f(\tilde{g}(\tilde{h}(z_t)), \tilde{g}(z_t), \tilde{h}(z_t), z_t, \eta_{t+1}) \right] \approx 0. \tag{19}$$

At $z = \hat{z}_{t|t-1}$, in fact, at any z, the functions $g(z)$ and $h(z)$ satisfy the equilibrium condition.

By the *Implicit Function Theorem*, if R is continuously differentiable and the Jacobian matrix with respect to the policies g and h is invertible, then the local approximate functions $\tilde{g}(z)$ and $\tilde{h}(z)$ exist and are differentiable in a neighborhood of $\hat{z}_{t|t-1}$. Since the residual function $R(z_t, \Theta)$ is zero $z_t = \hat{z}_{t|t-1}$ for the true $g(z)$ and $h(z)$, a first-order approximation of $g(z_t)$ and $h(z_t)$ using the Taylor Projection method is identical to solving for the local linear function that satisfies the residual function at $z_t = \hat{z}_{t|t-1}$.

Consequently, in this specific case where g and h are known, the Extended Kalman Filter and the Taylor Projection-based filter yield the same filtering equations. This follows because the EKF relies on local linearization of the policy and transition functions, which aligns precisely with the Taylor expansion obtained from the residual function. Note that there is one small difference in the timing in our Algorithm 1 and the EKF, that is, in EKF, T is linearized around $\hat{s}_{t|t}$ and Z is linearized around $\hat{s}_{t|t-1}$, while, for computational efficiency, we compute the local linear model solution at $\hat{s}_{t|t-1}$.

This is an important insight, because it implies that *without knowing (or having to solve for) the true solution $g(z)$ and $h(z)$*, the Taylor Projection-based filter is *as good* as knowing the true global model solution, and then filtering using the EKF.

EKF in practice A key question arising from this result is why one would prefer local approximations over an approximate global solution in practice. First, computing a global solution with the Extended Kalman Filter (EKF) is costly, often taking several minutes per parameter set (e.g., three minutes in Gust et al. (2017)), repeated for each sampler draw. Second, global solutions may fail to be accurate at all points in the state space, as policies are only guaranteed to satisfy equilibrium conditions at a finite set of nodes. More importantly, EKF's accuracy depends on the policy's derivative, which polynomial basis functions may approximate poorly, whereas local linear approximations ensure derivative accuracy by construction. Thus, while our equivalence result holds for the true global solution, in practice, global solutions are only approximations. Our algorithm may therefore be both faster and more accurate.

3 Monte Carlo: Filtering and Estimation of the DMP Model

In this section, we compare the performance of our proposed estimation framework to existing methods using simulations of the Diamond-Mortensen-Pissarides model. This model is known to have significant nonlinear dynamics (Petrosky-Nadeau and Zhang, 2017), making it a natural laboratory for the proposed method. We show that local linear approximation methods lead to highly accurate solutions, and, moreover, full-information estimation of the model with the proposed method achieves the same (or better) accuracy as a global solution coupled with particle filtering at a fraction of the computational cost.

3.1 Model Description

We only briefly describe the model environment, as the model is standard. The only non-standard assumption is the one made with respect to the timing of separations and hires. Following the literature on labor search in NK models (Christiano et al., 2016), we assume workers who lose their jobs at the beginning of the period can search within the period for a new job. This assumption is typically justified as a way of making low-frequency (quarterly) NK models conform with labor search where most unemployment spell last only a few weeks.[7]

[7] According to the estimate of Ahn and Hamilton (2022), two-thirds of workers exit unemployment within the first quarter of an unemployment spell.

Firms maximize the present discounted value of profit taking wages as given

$$\mathbb{E}_0 \left[\sum_{t=1}^{\infty} \beta^t \left\{ (Z_t - W_t) N_t - \kappa V_t \right\} \right]$$

subject to

$$N_t = (1 - \delta) N_{t-1} + q_t V_t,$$

where the flow payoff is output $Z_t N_t$, net of wage expenditures $W_t N_t$ and vacancy posting costs $\kappa V_t(j)$, δ is the job destruction rate, and q_t the vacancy filling rate. In equilibrium, the Nash wage is given by $W_t = \eta Z_t + (1 - \eta)\nu$, where η is the worker's bargaining weight, and ν is the outside option of the worker. This leads to job creation condition

$$\frac{\kappa}{q_t} = (1 - \eta)(Z_t - \nu) + (1 - \delta)\beta E_t \left[\frac{\kappa}{q_{t+1}} \right],$$

which is the sole equilibrium condition in the model. We assume productivity is stochastic, and log productivity, denoted z_t, follows an AR(1):

$$z_{t+1} = \rho_z z_t + \varepsilon_{t+1}.$$

3.2 Model Solution

The DMP model above has one state (TFP, z_t) and one policy to solve for: market tightness $\theta_t = g(z_t)$. In the local linear approximation, we approximate the policy function by:

$$\theta_t = \Gamma_1 + \Gamma_2 z_t$$

which implies $\theta_{t+1} = \Gamma_1 + \Gamma_2 \rho_z z_t + \Gamma_2 \varepsilon_{t+1}$ by iterating the law of motion for z_t one period forward.

The residual functions for the DMP model, used to solve for the local policy parameters, follow directly from the job creation condition in Equations (3.1), and are given by:

$$\begin{aligned} R(z, \Gamma)|_{z=z_t} &= \frac{\kappa}{q(\theta_t)} - (1 - \eta)(e^{z_t} - b) - \beta(1 - \delta)\mathbb{E}_t \left[\frac{\kappa}{q(\theta_{t+1})} \right] \\ \frac{\partial R(z, \Gamma)}{\partial z}|_{z=z_t} &= \frac{-\kappa q'(\theta_t)}{q(\theta_t)^2} \Gamma_2 - (1 - \eta) e^{z_t} + \beta(1 - \delta)\rho_z \Gamma_2 \rho_z \mathbb{E}_t \left[\frac{\kappa q'(\theta_t)}{q(\theta_t)^2} \right] \end{aligned}$$

This implies two equations in two unknowns Γ_1, Γ_2, which can be solved for numerically.

Figure 1: Comparison of log-linearization, global model solution, and dynamic Taylor projection for the DMP model.

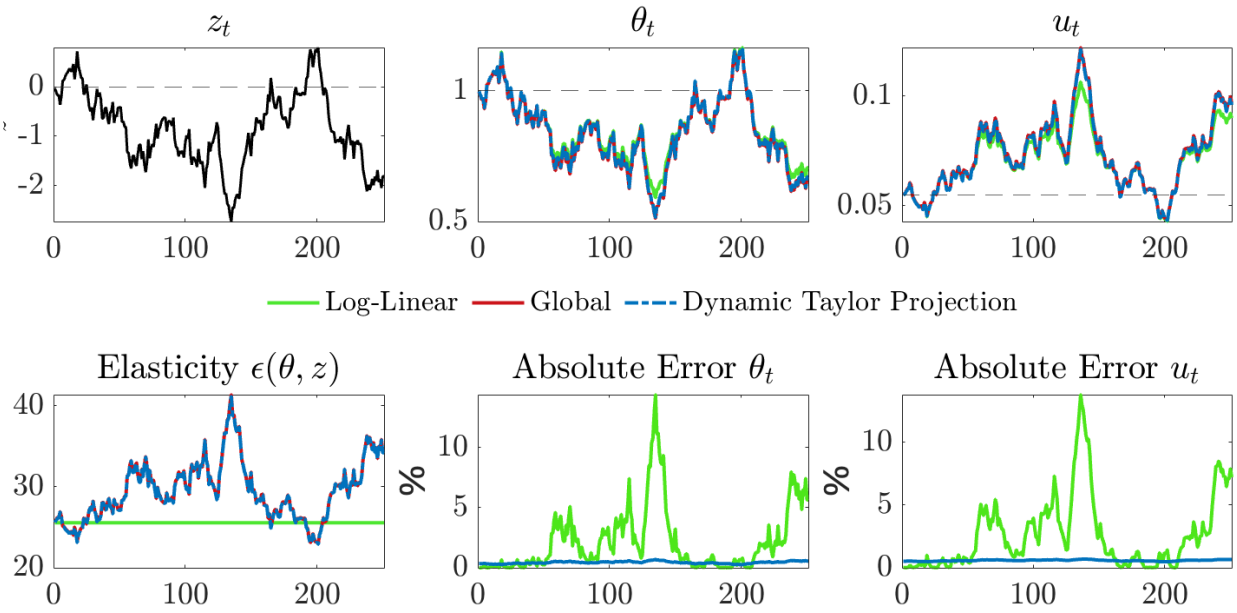


Figure 1 shows how a global model solution, approximating the unknown policy function by projection onto a set of polynomial basis functions, compared to a dynamic Taylor projection that computes the local linear approximation at each point of the solution path, and how these both compare to a log-linear model solution. The top row shows simulated paths for TFP, which are the same for all three methods, and the implied market tightness and unemployment rate. As can be seen, the simulation from the global model solution and dynamic Taylor projection follow each other closely. The log-linear solution deviates considerably, as measured by the two panels in the bottom row, showing the absolute error compared to the global model solution in market tightness and the unemployment rate, which can be above 10% for the log-linear solution, while for the dynamic Taylor projection, is always low.

The first panel in the second row shows that the local linear model solution also accurately tracks a key statistic of the DMP model: time-variability in the elasticity of market tightness and productivity. In a log-linear model solution, this elasticity is constant, since risk does not affect elasticities. Note that even in a second-order perturbation, this elasticity would be constant (Schmitt-Grohé and Uribe, 2004), because uncertainty only shifts the constant in the decision rule in a second order perturbation, and does not affect elastici-

ties. Concluding, local linear approximations are a highly accurate and computationally efficient alternative to global model solutions.

3.3 State-Space Representation

To make explicit how the Taylor projection solution maps into a linear state space model, assume we observe market tightness and wages, with measurement errors. Our local linear model solution around z is given by:

$$\theta_t = \Gamma_{1,z} + \Gamma_{2,z} z_t$$

and w follows as:

$$w_t = \eta z_t + (1 - \eta) b.$$

This implies that the state-space representation follows as:

$$\begin{pmatrix} \theta_t^{\text{obs}} \\ w_t^{\text{obs}} \end{pmatrix} = \begin{bmatrix} \Gamma_{2,z} \\ \eta \end{bmatrix} z_t + \begin{pmatrix} \Gamma_{1,z} \\ (1-\eta) b \end{pmatrix} + \varepsilon_t, \quad \varepsilon_t \sim \left(0,\ \text{diag}(\sigma^2_{e,\theta}, \sigma^2_{e,w})\right) \tag{20}$$

$$z_{t+1} = \rho_z z_t + \eta_t, \quad \eta_t \sim (0, \sigma_z^2). \tag{21}$$

We can then use Algorithm 1 to filter the underlying states and evaluate the likelihood of this model.

3.4 Monte Carlo

In this subsection, we present a simulation experiment based on 1,000 simulated datasets for two different lengths: $T = 200$, which is comparable to the data we use when we estimate the NKDMP model, and $T = 1000$ to provide some insight into asymptotic behavior. The experiment uses the DMP model presented above. For the first set of results, we assume we observe market tightness with measurement error which has a standard error equal to 25% of the standard deviation of the true underlying variable.

The experiment first solves the DMP model using a global solution method and generates simulated data from this solution. Then, it applies four different solution plus filtering approaches:

1. Linear perturbation with a standard Kalman filter (KF).
2. Global solution method with a particle filter (PF).

3. Taylor Projection (TP) with the time-varying Kalman filter (TV-KF) in Algorithm 1.

4. Global solution method with Extended Kalman filter (EKF)

We fix the structural model parameters to their true values (see Table 1 notes), and our goal is to assess how well each method recovers the unobserved states from the simulated data. Table 1 evaluate performance by comparing the R-squared (R^2) of the filtered states with the true states, along with the mean squared error (MSE) and mean absolute error (MAE). Additionally, the table reports computation times for each approach.

Table 1: Comparing Solution and Filtering Methods for the DMP model. MSE is scaled by the (unconditional) variance of the variable, MAE by the standard deviation.

	Linear + KF	Global + EKF	Global + PF			TP + TV-KF
Particles:			200	2,000	20,000	
T = 200						
R^2 Market Tightness	0.959	0.962	0.950	0.951	0.952	0.962
R^2 TFP	0.954	0.961	0.949	0.951	0.951	0.961
MSE Market Tightness	0.040	0.037	0.048	0.047	0.047	0.037
MSE TFP	0.066	0.020	0.026	0.025	0.025	0.020
MAE Market Tightness	0.157	0.154	0.160	0.158	0.158	0.154
MAE TFP	0.176	0.110	0.117	0.114	0.114	0.110
Computation time (sec)	0.001	0.101	0.148	0.564	4.523	0.007
T = 1,000						
R^2 Market Tightness	0.964	0.968	0.965	0.966	0.967	0.968
R^2 TFP	0.949	0.967	0.965	0.966	0.966	0.967
1e3 × MSE Market Tightness	0.035	0.031	0.033	0.032	0.032	0.031
1e6 × MSE TFP	0.077	0.028	0.030	0.029	0.029	0.028
10 × MAE Market Tightness	0.146	0.140	0.143	0.140	0.140	0.140
1e3 × MAE TFP	0.193	0.133	0.137	0.134	0.133	0.133
Computation time (sec)	0.008	0.109	0.359	2.487	22.62	0.032

Note: Calibration: $r = 0.04$, $\beta = \left(\frac{1}{1+r}\right)^{1/4}$, $\alpha = 0.7$, $\rho_z = 0.985$, σ_z=0.0015, $\eta = 0.5$, $b = 0.94$, $n_{ss} = 0.945$, $q_{ss} = 0.7$, $\theta_{ss} = 1$.

Focusing on computation time, for $T = 1,000$, Table 1 shows that TP+TV-KF is about three times slower than Linear+KF, while Global+PF is several orders of magnitude slower than TP+TV-KF. Using a global model solution in combination with EKF is about three times as slow for $T = 1,000$. In terms of accuracy, for low T, TP+TV-KF consistently outperforms both the global model + PF and the linear model + KF, across all three metrics. Confirming our theory, TP+TV-KF and Global+EKF have the same accuracy metrics. For larger T, Global+PF with a sufficient number of particles does improve and approaches

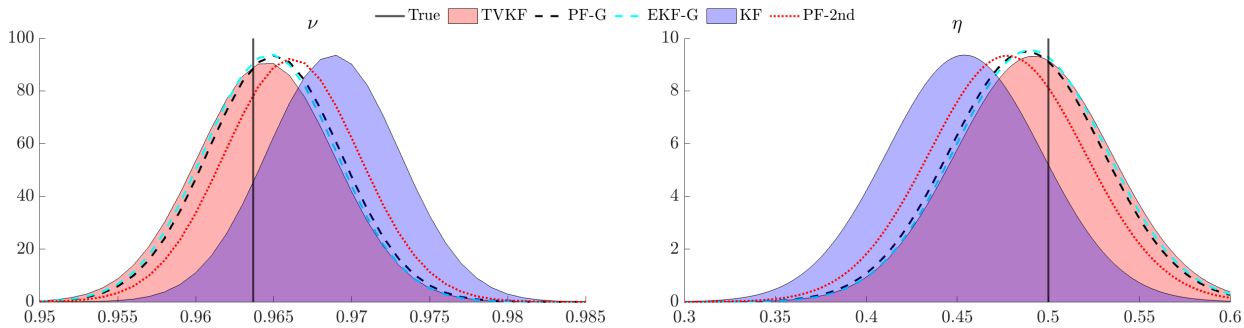
the accuracy of TP+TV-KF. For all sample sizes, Linear+KF performs considerably worse than the other methods. We conclude that the combination of Taylor Projections and the Time-Varying Kalman Filter is an accurate and computationally efficient solution and filtering approach.

3.5 Comparing Posteriors

Next, this subsection compares posteriors when the above-described filters are used in a Bayesian estimation routine with a Random Walk Metropolis Hastings algorithm for the posterior draws. We simulate a data set of length $T = 500$ from the global model solution parameterized as in the previous subsection. We assume we observe both market tightness and wages, with market tightness with measurement error standard deviation equal to 30% of the standard deviation of the simulated data series, and for wages 50%. In addition to the four estimation routines above, we also add a second-order perturbation of the DMP model, estimated using the particle filter.[8]

Focusing on economic parameters, Figure 2 shows the posterior distribution for the outside option ν and the bargaining power η. Both have a uniform prior $U[0, 1]$. For both parameters, the Kalman filter estimates are biased and the posterior distribution is shifted. The posterior distributions obtained from TP+TV-KF, Global+PF and Global+EKF closely align, and are close to the true value. A second-order perturbation filtered with particle filtering (red dotted line) only brings us half way from the biased linearized model parameter estimate to the true parameter, and is still biased, although less than the linear model.

Figure 2: Comparing posteriors for ν (outside option) and η (bargaining power) for the time-varying Kalman filter of Algorithm 1 (pink area), the Particle Filter + global model solution (black dash), Extended Kalman filter with global model solution (cyan dash), the linearized model with Kalman filter (blue area), and a second order perturbation with particle filter (red dotted).



[8]We use the implementation in Dynare.

4 Nonlinearities in the Three-Equation New Keynesian Model

4.1 Model Description

We closely follow the three-equation model in Gali (2015), and keep the description short, providing additional details in the Appendix on both the model and solution method.

Households Households supply labor, save in nominal bonds, and consume. A representative infinitely lived household maximizes the expected discounted sum of utilities

$$\mathbb{E}_0 \left[\sum_{t=0}^{\infty} \beta^t D_t U\left(C_t, N_t\right) \right]$$

subject to a sequence of budget constraints $P_t C_t + B_t = R_{t-1} B_{t-1} + P_t W_t N_t + T_t$, where C_t is consumption of the final good, B_t is an uncontingent nominal bond, R_{t-1} is the nominal interest rate, W_t is the real wage, and T_t contains dividends from firms net of taxes and transfers from the government. We assume utility has the following form

$$U\left(C_t, N_t\right) = \begin{cases} \frac{C_t^{1-\tau}-1}{1-\tau} - \chi \frac{N_t^{1+\eta}}{1+\eta}, \text{ if } \tau \neq 1 \\ \log(C_t) - \chi \frac{N_t^{1+\eta}}{1+\eta}, \text{ if } \tau = 1. \end{cases}$$

$d_t = \log(D_t)$ is a random discount factor shock to the utility of consumption and follows an AR(1):

$$d_{t+1} = \rho_d d_t + \varepsilon_t^d, \quad \varepsilon_t^d \sim N(0, \sigma_d^2).$$

Firms We assume perfectly competitive final good firms combine a continuum of intermediate goods $j \in [0,1]$. Each intermediate good j is produced by a monopolist with technology $Y_t(j) = A_t N_t(j)$ where A_t is an aggregate technology process common to all firms. These firms choose prices $P_t(j)$ and labor inputs $N_t(j)$ to maximize the present discounted value of profit

$$\mathbb{E}_0 \left[Q_{0,t} \left\{ \frac{P_t(j)}{P_t} A_t N_t(j) - W_t N_t(j) - \frac{\phi}{2} \left(\frac{P_t(j)}{P_{t-1}(j)} - \Pi \right)^2 Y_t \right\} \right], \quad \text{s.t. } A_t N_t(j) = \left(\frac{P_t(j)}{P_t} \right)^{-1/\gamma} Y_t,$$

where $\frac{\phi}{2} \left(\frac{P_t(j)}{P_{t-1}(j)} - \Pi \right)^2 Y_t$ reflects the Rotemberg price-adjustment cost. $a_t = \log A_t$ follows an AR(1) process. Π is steady state inflation.

Government The government levies lump-sum taxes and runs a balanced budget. The monetary authority follows a Taylor type rule

$$\frac{R_t}{R} = \left(\frac{\Pi_t}{\Pi}\right)^{\phi_\pi} \left(\frac{Y_t}{Y}\right)^{\phi_y} e^{m_t}, \qquad m_{t+1} = \rho_m m_t + \varepsilon_t^m, \;\; \varepsilon_t^m \sim N(0, \sigma_m^2),$$

where m_t is an exogenous monetary policy shock that follows an AR(1).

Equilibrium A minimal state representation consists of states $\mathbb{S} = \{a_t, d_t, m_t\}$ and policies $\{\Pi(\mathbb{S}), N(\mathbb{S})\}$ defined through the equilibrium conditions (substituting market clearing conditions where appropriate)

$$\begin{aligned}
\text{Euler/IS}: \; & 1 = \beta \mathbb{E}_t \left[e^{(\rho_d - 1) d_t + \epsilon_{t+1}^d} \left(\frac{N_{t+1}}{N_t} e^{(\rho_a - 1) a_t + \epsilon_{t+1}^a} \right)^{-\tau} \frac{R_t}{\Pi_{t+1}} \right] \\
\text{Pricing/NK-Phillips}: \; & \frac{1}{\gamma} \left(1 - \chi N_t^{\eta+\tau} e^{(\tau-1) a_t} \right) = 1 - \phi \left(\Pi_t - \Pi \right) \Pi_t \\
& \quad + \phi \beta \mathbb{E}_t \left[e^{(\rho_d - 1) d_t + \epsilon_{t+1}^d} \left(\frac{N_{t+1}}{N_t} e^{(\rho_a - 1) a_t + \epsilon_{t+1}^a} \right)^{1-\tau} \left(\Pi_{t+1} - \Pi \right) \Pi_{t+1} \right] \\
\text{Taylor Rule}: \; & \frac{R_t}{R} = \left(\frac{\Pi_t}{\Pi} \right)^{\phi_\pi} \left(\frac{N_t Z_t}{Y} \right)^{\phi_y} e^{m_t}
\end{aligned}$$

More details on the model and equilibrium derivation are provided in the Appendix E.

4.2 Model Solution

We solve the model above using local linear approximations, that is, Taylor Projections (Levintal, 2018) of first-order. Given the minimal state representation stated above, we need to solve for two policy functions:

$$g_\Pi(a_t, d_t, m_t; z) = \alpha_{0,z} + \alpha_{1,z} a_t + \alpha_{2,z} d_t + \alpha_{3,z} m_t$$

and

$$g_N(a_t, d_t, m_t; z) = \beta_{0,z} + \beta_{1,z} a_t + \beta_{2,z} d_t + \beta_{3,z} m_t,$$

where the coefficients $\alpha_0, \alpha_1, \alpha_2, \alpha_3, \beta_0, \beta_1, \beta_2, \beta_3$ are allowed to differ at each point of the state-space where the local approximation is computed, reflected by subscript z. In Appendix E, we show how expectation operators of equilibrium conditions can be solved in closed form.

4.3 State-Space Representation

The states of the model are given by $s_t = (a_t, d_t, m_t)$. The state-transition equation is not time-varying, and follows:

$$\begin{pmatrix} a_{t+1} \\ d_{t+1} \\ m_{t+1} \end{pmatrix} = \begin{pmatrix} \rho_a & 0 & 0 \\ 0 & \rho_d & 0 \\ 0 & 0 & \rho_m \end{pmatrix} \begin{pmatrix} a_t \\ d_t \\ m_t \end{pmatrix} + \begin{pmatrix} \varepsilon^a_{t+1} \\ \varepsilon^d_{t+1} \\ \varepsilon^m_{t+1} \end{pmatrix}, \qquad \begin{pmatrix} \varepsilon^a_t \\ \varepsilon^d_t \\ \varepsilon^m_t \end{pmatrix} \sim N\left(0, \text{diag}(\sigma_a^2, \sigma_d^2, \sigma_m^2)\right)$$

Assume we observe log output y_t^{obs}, log inflation π_t^{obs}, and log interest rates r_t^{obs}. Our observation equation, conditional on having solved the model at state z resulting in policy coefficients $\{\alpha_{i,z}\}_{i=0}^3$ and $\{\beta_{i,z}\}_{i=0}^3$, is given by:

$$\begin{pmatrix} y_t^{\text{obs}} \\ \pi_t^{\text{obs}} \\ r_t^{\text{obs}} \end{pmatrix} = \begin{pmatrix} \beta_{0,z} \\ (\pi_{ss} + \alpha_{0,z}) \\ (r_{ss} + \psi_\pi \alpha_{0,z} + \psi_y \beta_{0,z}) \end{pmatrix} + Z \begin{pmatrix} a_t \\ d_t \\ m_t \end{pmatrix} + \eta_t, \qquad \eta_t \sim N(0, \text{diag}(\sigma_y^{ME}, \sigma_\pi^{ME}, \sigma_r^{ME})^2)$$

$$\text{where } Z = \begin{pmatrix} \beta_{1,z} + 1 & \beta_{2,z} & \beta_{3,z} \\ \alpha_{1,z} & \alpha_{2,z} & \alpha_{3,z} \\ (\psi_\pi \alpha_{1,z} + \psi_y(\beta_{1,z} + 1)) & (\psi_\pi \alpha_{2,z} + \psi_y \beta_{2,z}) & (\psi_\pi \alpha_{3,z} + \psi_y \beta_{3,z} + 1) \end{pmatrix},$$

and σ_y^{ME}, σ_π^{ME} and σ_r^{ME} represent the measurement error standard deviations of log output, inflation and interest rates, respectively. Note that the bottom row in Z reflects how interest rates depend on both output and inflation through the monetary policy rule. This linear state-space representation allows us to solve and filter the model as in Algorithm 1.

4.4 Data

For estimation, we use logged real GDP-per-capita [9], detrended using the HP-filter with a smoothing parameter of 1,600. Inflation is quarterly inflation based on the GDP deflator[10] and the nominal rate is the quarterly equivalent of the annual federal funds rate[11]. The data are visualized in Figure 4. We estimate the model on the 1966:Q1-2007:Q4 sample.

[9] FRED: GDPC1 divided by FRED: CNP16OV
[10] FRED: GDPDEF
[11] FRED: DFF

4.5 Sampling and Run Time

Sampling We use a Random-Walk Metropolis Hastings sampler to obtain draws from the posterior. The proposal variance of the algorithm is initialized as the variance-covariance matrix of the loglinearized posterior draws, scaled to obtain an acceptance rate of 30%. We use the same priors as for the linear model, presented in Table 2. We calibrate a subset of parameters: $\gamma = 0.1$, $\phi_p = 100$ (based on Gust et al. (2017)) and $\eta = 3$.

Runtime In Matlab, on a standard laptop without parallelization, it takes 9 minutes and 20 seconds to get 100,000 draws from the nonlinear model, about 0.0056 seconds per draw.[12] This is less than twice as long as estimating the linear model in Dynare (Adjemian et al., 2024), which takes five and a half minutes.

4.6 Estimation Results

Comparing Linear and Nonlinear Estimates Table 2 and Figure 3 report the priors – which are common across both the linear model and nonlinear model – and the resulting posteriors for both the linear and nonlinear model estimates. For a subset of parameters, the linear and nonlinear model agree closely on the shape and location of the posterior distribution, such as the Taylor rule coefficient for output ψ_y (0.2 and 0.18 respectively for linear and nonlinear with comparable credible intervals), the volatility of discount factor shocks σ_d (0.0028) and the steady state inflation π_{ss} and interest rate r_{ss}.

In other cases, the posterior shifts, resulting in considerably different posteriors and point estimates. Focusing on the economic parameters, the Taylor rule parameter ψ_π increases from 2.5 to 2.9, and risk aversion τ decreases from 2.14 to 1.47 in the nonlinear model, both of which are economically meaningful changes. Note that for the nonlinear model, the estimates for the measurement error standard deviation in the nonlinear model are lower, in particular for output and interest rate, indicating a better fit of the nonlinear model to the data.

Figure 4 shows both data and filtered states, comparing the states from the linear and nonlinear model. The filtered series for total factor productivity and the discount factor look comparable, but the monetary policy shock series differs more strongly between the two model and estimation approaches, particularly for the period from the mid 70s to the mid 80s, where the nonlinear model uncovers larger negative shocks.

[12] Computations are done on a Apple Macbook Pro with an Apple M3 Max processor and 64GB RAM.

Table 2: Prior mean and standard deviation, posterior mean and 90% CI

Parameter	Prior	Linear Posterior		Nonlinear Posterior	
	(Mean, Std.)	Mean	[5%, 95%]	Mean	[5%, 95%]
		Economic Parameters			
τ	G (2, 0.5)	2.14	[1.63, 2.59]	1.47	[0.81, 2.24]
ψ_y	G (0.75, 0.25)	0.20	[0.11, 0.30]	0.18	[0.09, 0.29]
ψ_π	G (1.5, 0.25)	2.50	[2.29, 2.73]	2.89	[2.52, 3.29]
		Persistences of shocks			
ρ_m	B (0.7, 0.15)	0.945	[0.910, 0.974]	0.961	[0.929, 0.986]
ρ_d	B (0.7, 0.15)	0.943	[0.913, 0.963]	0.939	[0.909, 0.966]
ρ_a	B (0.7, 0.15)	0.984	[0.966, 0.996]	0.978	[0.944, 0.996]
		Standard deviations of shocks			
$100\times\sigma_m$	IG (0.5, 1)	0.24	[0.19, 0.30]	0.27	[0.20, 0.35]
$10\times\sigma_d$	IG (0.5, 5)	0.28	[0.19, 0.38]	0.28	[0.18, 0.44]
$100\times\sigma_a$	IG (1, 1)	0.38	[0.35, 0.43]	0.35	[0.30, 0.40]
		Steady states			
π_{ss}	G (0.018,0.01)	0.009	[0.007, 0.011]	0.008	[0.004, 0.012]
r_{ss}	G (0.054,0.02)	0.015	[0.012, 0.017]	0.014	[0.009, 0.019]
		Measurement error			
$100\times\sigma_y^{ME}$	IG(0.21, 200)	0.08	[0.05, 0.11]	0.05	[0.03, 0.09]
$100\times\sigma_\pi^{ME}$	IG(0.18, 200)	0.19	[0.17, 0.22]	0.20	[0.17, 0.22]
$100\times\sigma_r^{ME}$	IG(0.24, 200)	0.07	[0.05, 0.10]	0.05	[0.03, 0.07]

Note: G is Gamma, IG is inverse Gamma, B is Beta.

State-Dependence in the Three-Equation New Keynesian Model An important difference between the linearized and nonlinear model is the state-dependence in the nonlinear model solution. Figure 5 highlights significant time variation in the impulse response functions to a monetary policy shock and a discount factor shock, comparing shocks occurring in 1982 versus 2006. The key difference between these periods is the discount factor (see Figure 4). We find that the initial impact of both monetary policy and discount factor shocks on output was approximately twice as large in 1982 as in 2006. We do not find evidence of state dependence in total factor productivity (TFP) in this model, and thus, do not visualize those IRFs. The figure also shows the impulse response function for the estimated linear model, which does not depend on the state of the economy.

Figure 3: Priors and Posteriors

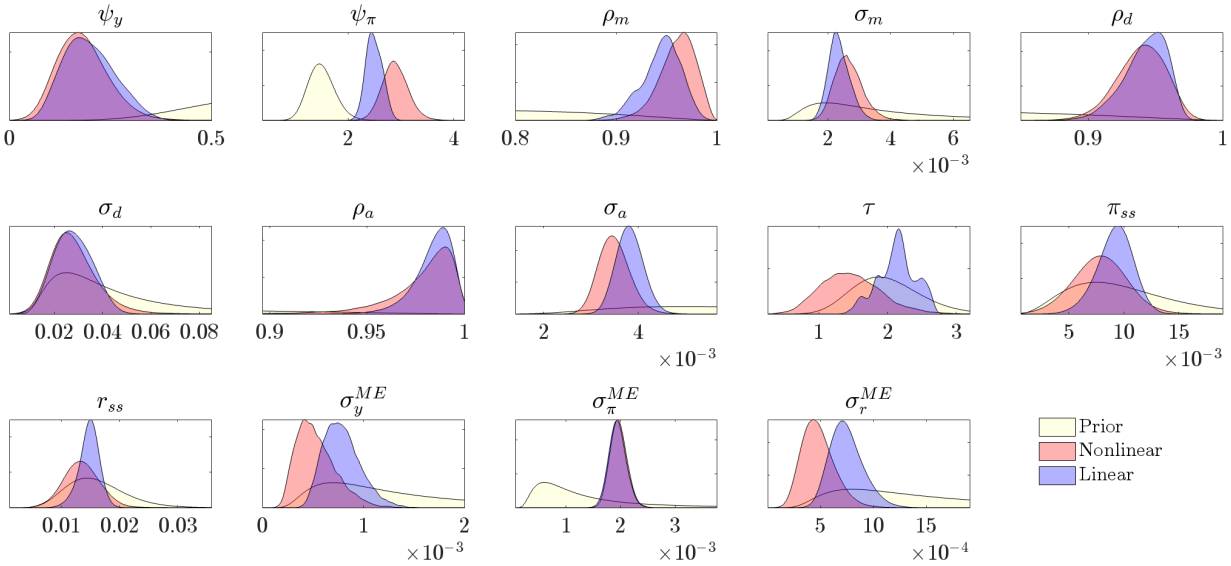
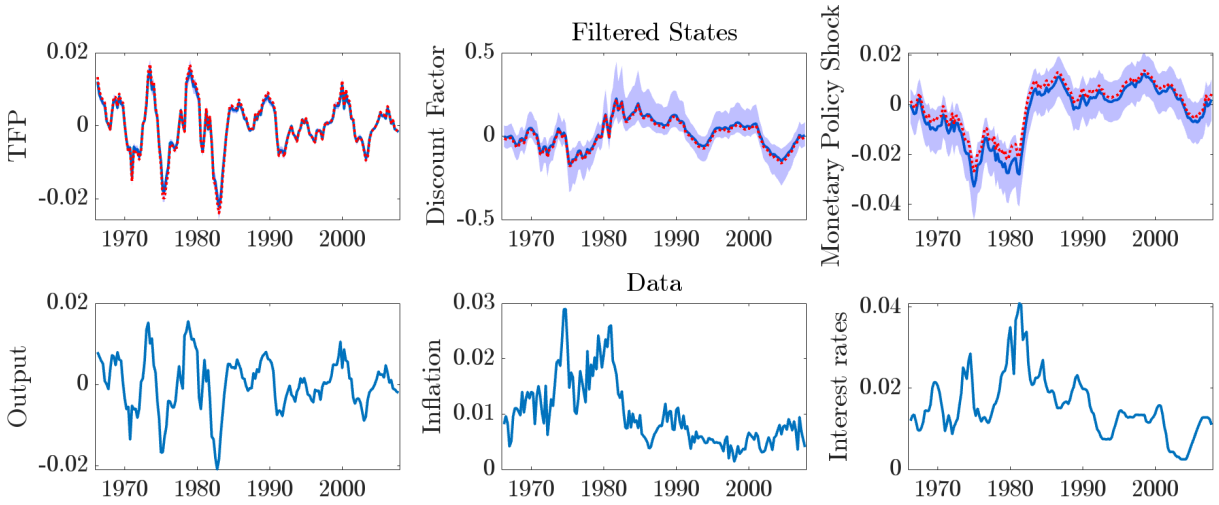


Figure 4: Filtered States (Linear (red dots) versus Nonlinear (blue solid, with 95% CI interval)) and Data



Note: Credible intervals only reflects parameter uncertainty, not uncertainty about the state.

State dependence in the response to monetary policy shocks is particularly relevant for policymakers, as it implies variation in the output-inflation trade-off. Figure 6 illustrates this trade-off by computing the cumulative impulse response functions (IRFs) for inflation and output following a monetary policy shock, as well as their ratio, which we use as a measure of the trade-off. The figure shows that the output-inflation trade-off peaked in the early 1980s at close to 0.09 before declining to almost as low as 0.07 mid 00s. Due to parameter uncertainty, this decline is not statistically significant (not visualized), but the

decline aligns with the notion that the Phillips curve has flattened from the 1980s to the early 2000s, consistent with findings from Stock and Watson (2020) (albeit less extreme) and Hazell et al. (2022). Importantly, this result does not require introducing additional frictions or time-varying parameters, but emerges naturally by solving and estimating the model nonlinearly. The model attributes the observed flattening to a decline in the discount factor over this period.

Figure 5: State Dependence in Impulse Response Functions

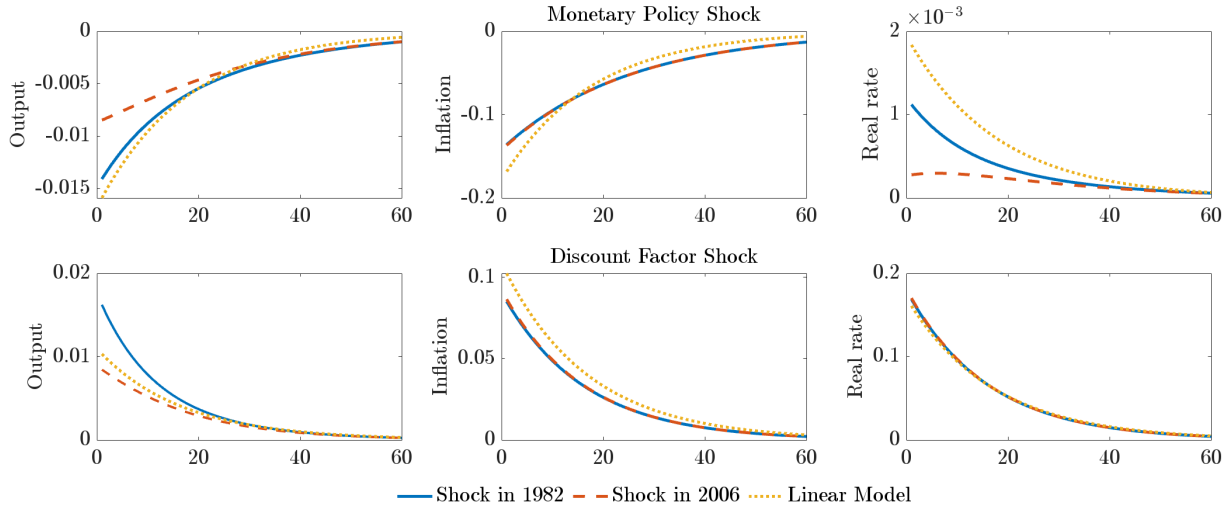
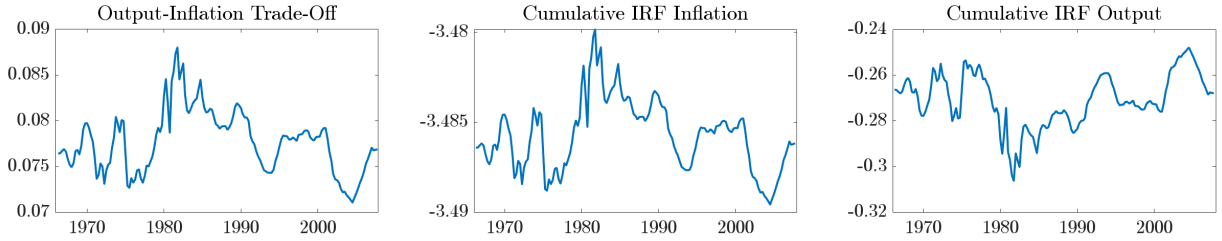


Figure 6: Time-Varying Monetary Policy Shock Transmission in the Three-Equation New Keynesian Model



5 A New Keynesian Model with Labor Search

In this section, we present a small New Keynesian (NK) model with search frictions, following the Diamond-Mortensen-Pissarides (DMP) framework. The model illustrates how the strength of monetary policy transmission depends on firms' flow surplus, leading to state-dependent effects of monetary policy. We provide intuition for this result by analytically log-linearizing the mode, showing that surplus scales the sensitivity to shocks. Additionally, the model provides theoretically grounded proxies for firm surplus, which we employ in our empirical analysis to test for the presence of such state dependence in

the data, which we do in Section 6. Furthermore, this model serves as the foundation for the more comprehensive NK-DMP framework developed at the end of Section 5 and estimated in Section 7.

5.1 Key Model Ingredients

Overview The economy consists of households that consume and supply labor, intermediate good producers that set prices and hire labor in a frictional labor market where workers seek to match with jobs, and final good producers that aggregate intermediate goods while taking prices as given. Wages are determined through Nash bargaining between workers and intermediate goods firms. The government sets the nominal interest rate according to an inertial Taylor rule.

Timing We follow the same timing assumption as in Section 3. Each model period consists of four sub-periods: (i) separations, (ii) search and matching, (iii) bargaining, and (iv) production and consumption/saving.

Households Households are composed of a continuum of members $i \in [0,1]$ who derive utility from consumption $c_t(i)$, and supply one unit of labor $n_t(i) \in \{0,1\}$ if employed and none if unemployed. The members of the household perfectly insure each other against variations in income due to unemployment. Hence, defining $C_t := \int c_t(i)di$, and $N_t := \int n_t(i)di$, households maximize:

$$\mathbb{E}_0 \left[\sum_{t=0}^{\infty} \beta^t \frac{C_t^{1-\tau} - 1}{1-\tau} \right],$$

subject to the budget constraint

$$P_t C_t + B_t = P_t W_t N_t + P_t(1 - N_t)\nu + R_{t-1} B_{t-1} + T_t,$$

and the law of motion for employment

$$N_t = (1-\delta)N_{t-1} + q_t V_t.$$

Here β is the discount factor, $1/\tau$ is the intertemporal elasticity of substitution, P_t is the price of the final good, B_t denotes one-period risk-free bonds with gross return R_t, and T_t denotes lump sum taxes net of profits transferred from firms. W_t are real wages, ν is the resources provided by the unemployed (e.g., unemployment benefits and home

production). The law of motion for employment depends on the exogenous separation rate δ and the number of new hires $q_t V_t$ made by firms which the household takes as given, with V_t the number of vacancies and q_t the vacancy filling rate

Defining the surplus to the household of employment S_t^h using the envelope condition, we obtain:

$$S_t^h = W_t - \nu + (1-\delta)E_t\left[Q_{t,t+1}S_{t+1}^h\right].$$

which denotes the present value of a marginal employed household member.

Search and Matching The number of aggregates matches is determined by a constant return to scale matching function $M_t = M(V_t, S_t)$ where V_t is aggregate vacancies and S_t is the number of unmatched workers searching for jobs. Given the timing assumption, the mass of unmatched workers in the search stage is given by $S_t = 1 - N_{t-1} + \delta N_{t-1} = 1 - (1-\delta)N_{t-1}$, that is the workers who were not matched at the end of the previous production stage plus those who incurred an involuntary separation at the beginning of the period. The probability a vacancy contacts workers can be summarized by the market tightness $\theta_t = V_t/S_t$ as $q_t = M_t/V_t = M\left(1, \theta_t^{-1}\right)$.

Final Goods Producers The finals good producer aggregates intermediate goods $Y_t(j)$, $j \in [0,1]$, using the technology:

$$Y_t = \left(\int_0^1 Y_t(j)^{1-\gamma} dj\right)^{\frac{1}{1-\gamma}}.$$

The representative firm maximizes profits taking input prices $P_t(j)$ and output prices P_t as given. Profit maximization implies that the demand for input j is given by:

$$Y_t(j) = \left(\frac{P_t(j)}{P_t}\right)^{-\frac{1}{\gamma}} Y_t.$$

Intermediate Goods Producers There is a continuum $j \in [0,1]$ of identical monopolistic intermediate goods producers, with production technology

$$Y_t(j) = Z_t N_t(j)$$

where Z_t is a neutral technology shock, and $N_t(j)$ is the quantity of labor. These firms are monopolists in the product market and hire in frictional labor markets. Price adjustments are subject to a Rotemberg (1982) quadratic adjustment cost, just like in Section 4.

Firms hire labor in a frictional labor market by posting vacancies at a fixed cost κ. Hence, the firm's problem is to choose employment $N_t(j)$, vacancies $V_t(j)$, and prices $P_t(j)$ to maximize the present value of real profits discounted by $Q_{0,t}$:

$$\Pi_0(j) = \mathbb{E}_0 \sum_{t=0}^{\infty} Q_{0,t} \left\{ \left(\frac{P_t(j)}{P_t} Z_t - W_t \right) N_t(j) - \kappa V_t(j) - AC_t(j) \right\}.$$

subject to

$$\begin{aligned} Z_t N_t(j) &= \left(\frac{P_t(j)}{P_t} \right)^{-\frac{1}{\gamma}} Y_t, && [\omega_t] \\ N_t(j) &= (1-\delta) N_{t-1}(j) + q_t V_t(j). && [\mu_t] \end{aligned}$$

where the first constraint implies that the choice of output $Y_t(j) = Z_t N_t(j)$ and prices $P_t(j)$ are constrained to lie on the firms' product demand curves. The multiplier on this constraint is given by ω_t. This leads to both an explicit cost of labor the real wage W_t and an implicit cost ω_t as hiring a marginal worker – all else equal – leads to a reduction in prices. The second constraint is the law of motion for employment at the firm and the multiplier μ_t represents the value of a marginal worker to the firm.

Wage Bargaining The wage is determined by the Nash sharing rule

$$\eta \mu_t = (1-\eta) S_t^h.$$

where η is the workers' bargaining weight. This leads to the following expression for the real wage

$$W_t = \eta Z_t (1 - \omega_t) + (1-\eta) \nu$$

where ν is the flow value of non-employment and ω_t is the implicit marginal cost of hiring.

Government Monetary policy is determined by an inertial Taylor Rule for the nominal interest rate:

$$\frac{R_t}{\bar{R}} = \left[\left(\frac{\Pi_t}{\bar{\Pi}} \right)^{\psi_1} \left(\frac{Y_t}{Y_{t-1}} \right)^{\psi_2} \right]^{1-\rho_R} \left(\frac{R_{t-1}}{\bar{R}} \right)^{\rho_R} e^{\epsilon_{R,t}}$$

where R_t is the nominal interest rate. The systematic component of monetary policy reacts to the state of the economy, $\Pi_t = P_t/P_{t-1}$ is inflation, Y_t is output, and $\epsilon_{R,t}$ is the shock. The government levies lump-sum taxes (or provides a subsidy) to run a balanced budget every period.

Equilibrium Conditions We assume vacancy costs and adjustment costs are paid in lump-sum fashion to households, so market clearing implies $C_t = Y_t$. This leads to the following Euler equation

$$1 = \beta \mathbb{E}_t \left[\left(\frac{Y_{t+1}}{Y_t} \right)^{-\tau} \frac{R_t}{\Pi_{t+1}} \right].$$

In a symmetric equilibrium all firms set the same prices $P_t = P_t(j)$ and choose the same level of employment $N_t(j) = N_t$ and vacancies $V_t(j) = V_t$ leading to the following pricing equation

$$\frac{\omega_t}{\gamma} = 1 - \phi(\Pi_t - \bar{\Pi})\Pi_t + \phi\beta \mathbb{E}_t \left[\left(\frac{Y_{t+1}}{Y_t} \right)^{1-\tau} (\Pi_{t+1} - \bar{\Pi})\Pi_{t+1} \right].$$

Similarly, optimal vacancy posting and the expression for the Nash wage leads to the following job-creation condition

$$\frac{\kappa}{q_t} = (1-\eta)\left[(1-\omega_t)Z_t - \nu\right] + \beta(1-\delta)\mathbb{E}_t \left[\left(\frac{Y_{t+1}}{Y_t} \right)^{-\tau} \frac{\kappa}{q_{t+1}} \right]$$

To close the model, the interest rate rule and law of motion for employment are given by

$$\frac{R_t}{\bar{R}} = \left[\left(\frac{\Pi_t}{\bar{\Pi}} \right)^{\psi_1} \left(\frac{Y_t}{Y_{t-1}} \right)^{\psi_2} \right]^{1-\rho_R} \left(\frac{R_{t-1}}{\bar{R}} \right)^{\rho_R} e^{\epsilon_{R,t}}$$

$$N_t = (1-\delta)N_{t-1} + \underbrace{q_t \theta_t \left[1 - (1-\delta)N_{t-1}\right]}_{= q_t V_t}$$

5.2 State-Dependence

We use the system of log-linearized conditions to think about the deterministic response of the system to a one-time monetary shock $\epsilon_{R,t}$, that is, the perfect foresight path. Details on the equilibrium conditions and the derivation of the log-linear system are provided in Appendix D. In this framework, total factor productivity is at steady state, hence $\hat{z}_t = 0$, where the $\hat{\cdot}$ notation denotes a variable in log-deviation from the steady state. This gives

us a reduced system of equations (where we omit expectation operators as this is the perfect foresight response):

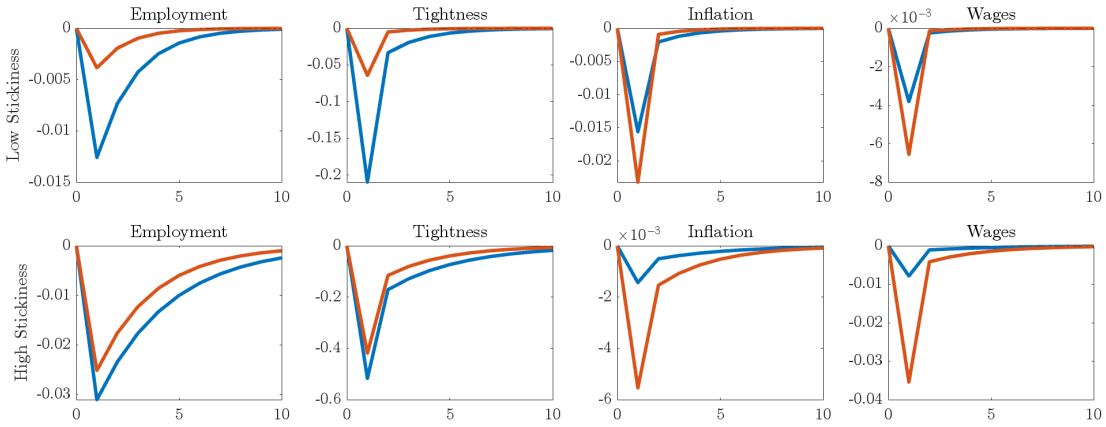
$$\begin{aligned}
\text{Euler/IS:}\quad & \hat{n}_{t+1} = \hat{n}_t + \frac{1}{\tau}\left[\hat{r}_t - \hat{\pi}_{t+1}\right] \\
\text{Pricing/NK-Phillips:}\quad & \hat{\pi}_t = \beta\hat{\pi}_{t+1} - \frac{1}{\phi}\hat{\omega}_t \\
\text{Job-Creation:}\quad & \hat{q}_t = \frac{\gamma(1-\beta(1-\delta))}{(1-\eta)(1-\gamma-\nu)}\hat{\omega}_t + (1-\delta)\beta\left[\hat{q}_{t+1} + \hat{r}_t - \hat{\pi}_{t+1}\right] \\
\text{Taylor Rule:}\quad & \hat{r}_t = (1-\rho_R)\left[\psi_1\hat{\pi}_t + \psi_2(\hat{n}_t - \hat{n}_{t-1})\right] + \rho_R\hat{r}_{t-1} + \epsilon_{R,t} \\
\text{LOM:}\quad & \hat{n}_t = (1-\delta)\hat{n}_{t-1} + \delta\left(\hat{q}_t + \hat{v}_t\right)
\end{aligned}$$

As evident from the log-linearized job creation condition, the sensitivity of q_t to ω_t scales inversely with $(1-\eta)(1-\gamma-\nu)$, which represents the steady-state flow profit of the firm. This is closely related to the *fundamental surplus* concept in Ljungqvist and Sargent (2017). When the flow profit is small, shocks propagate more strongly to the vacancy-filling rate q_t, and vice versa. Since q_t determines market tightness, the same mechanism governs the propagation of shocks to market tightness and, consequently, employment and output. Given that inflation depends on $\hat{\omega}_t$ through the New Keynesian Phillips curve, this mechanism also drives state dependence in inflation. The strength of inflation's response to a monetary shock is influenced by the degree of price stickiness ϕ, as specified in the Rotemberg (1982) adjustment cost framework.

In a log-linearized NK-DMP model, the propagation mechanisms depend on steady-state profit $(1-\eta)(1-\gamma-\nu)$ for real variables and on price stickiness ϕ for inflation. However, these elasticities remain constant across different economic states. To accurately capture state dependence, we require a solution method that allows these elasticities to vary with the state of the economy. As we will demonstrate in Section 6, the nonlinear model solution exhibits significant state dependence.

Even in our log-linearized solution, however, we can illustrate this intuition by computing perfect foresight paths for a monetary policy shock around four different steady states: one economy with a low steady-state profit and another with a high steady-state profit, and then examining how these economies differ under varying levels of price stickiness. We visualize this in Figure 7. When prices are flexible, the model reveals strong state dependence in real variables (employment and market tightness), whereas price variables

Figure 7: Perfect foresight paths to a monetary policy shock in a low and high surplus steady state and a low and high price stickiness economy



(inflation and real wages) exhibit weaker state dependence. Increasing the degree of price stickiness reduces state dependence in real quantities while amplifying it in prices.

To summarize, an economy with a small surplus steady state exhibits larger responses to a monetary shock than one with a large surplus steady state. However, whether this state dependence primarily affects quantities or prices depends on the degree of price stickiness.

5.3 Model-Implied Proxies for Surplus

The simple NK-DMP model implies that the propagation of monetary shocks depends on the profitability of job creation. The job-creation condition equates the marginal cost of hiring, κ/q_t, to the present value of profits from a marginal hire. Following this logic, we identify three proxies for the state of the economy, which we examine in the empirical section.

1. **Marginal Cost of Hiring:** In the model, the marginal cost of hiring is given by κ/q_t, but in the data, q_t is not directly observed. However, assuming a constant returns to scale matching function, $f_t = \theta_t q_t$, where f_t is the job-finding rate and θ_t represents market tightness—both of which are observable. This relationship implies that the marginal cost of hiring is proportional to θ_t/f_t, which we use as our first proxy.

2. **Corporate Profits:** The value of job creation corresponds to the present value of profits obtained from a marginal hire. While this present value is not directly observable in the data, corporate profits are. In the data, we measure profits as the

ratio of total profits (value added net of employee compensation) to value added in the corporate sector.

3. **Total Factor Productivity (TFP):** In the model, when total factor productivity Z_t increases, the rigidity in real wages implied by the Nash bargaining rule causes wages to rise by less than one-to-one with the marginal product. This results in procyclical profits and procyclical job creation. A natural candidate for capturing the state of the economy is TFP.

Taken in isolation, each of these proxies has predictive power for state dependence if (i) the NK-DMP model is the data-generating process and (ii) the proxies are well measured. However, (i) is not strictly true, as any model is only an approximation of reality, and (ii) relies on the assumptions that vacancy costs are linear, that flow profit and the present value of profit are related, and that TFP can be reliably measured. To mitigate potential limitations associated with any single proxy, we examine the effects of monetary policy shocks by comparing results across all three proxies. To the extent that our empirical findings are consistent across all three proxies, we consider our results robust.

5.4 Quantitative Model

This section extends the simple NK-DMP model from Section 5.1 to include (i) a set of exogenous shocks, (ii) a zero lower bound for the nominal interest rate, and (iii) habit preferences. These extensions allow us to estimate the model using full-information methods on post-war U.S. data. Since the firms and wage bargaining protocol are identical to that in Section 5.1, we focus on the household and government sectors and refer to the previous section for details on the production side.

Households The economy is populated by a continuum of identical households $i \in [0, 1]$ who derive utility from consumption, and supply one unit of labor inelastically to the labor market. The preferences of the representative household are an equally weighted average of its members.

The welfare of household i is given by

$$\mathbb{E}_0 \left[\sum_{t=0}^{\infty} \beta^t D_t \frac{(C_{it} - bC_{t-1})^{1-\tau} - 1}{1-\tau} \right],$$

where b is a measure of external habits, β is the discount factor, D_t is a shock to intertemporal preferences, and $1/\tau$ is the intertemporal elasticity of substitution. The budget constraint and law of motion for employment are identical to those in the previous section.

The first-order condition with respect to consumption implies

$$\lambda_t = D_t \left(C_{it} - bC_{t-1}\right)^{-\tau},$$

where λ_t is the marginal utility of consumption. We define the stochastic discount factor used by firms as

$$Q_{t,t+1} = \beta \frac{\lambda_{t+1}}{\lambda_t}.$$

Government Monetary policy is determined by a Taylor Rule for the nominal interest rate subject to a ZLB constraint:

$$R_t = \max\left\{1, \tilde{R}_t e^{m_t}\right\},$$

where $\tilde{R}_t$ is the systematic component of monetary policy that reacts to the state of the economy, and m_t is the shock. We consider the following Taylor rule:

$$\tilde{R}_t = R \left(\frac{\Pi_t}{\bar{\Pi}}\right)^{\psi_\pi} \left(\frac{Y_t}{Y_{t-1}}\right)^{\psi_y}$$

The central bank responds to deviations in inflation and output from their targeted values, $\bar{\Pi}$, as well as to the growth rate of output. Note that the nominal interest rate is almost everywhere differentiable, except at the kink where the ZLB begins to bind. The local perturbation method we employ assumes that the equilibrium conditions of the model are differentiable in the state variables. To accommodate the ZLB, we smooth the kink using the softmax function

$$R_t = \zeta \log\left(e^{1/\zeta} + e^{\tilde{R}_t e^{m_t}/\zeta}\right),$$

where the parameter ζ determines how smooth the approximation is and has the property

$$\lim_{\zeta \to 0} R_t = \max\left\{1, \tilde{R}_t e^{m_t}\right\}.$$

Exogenous States

$$\ln D_t = \rho_d \ln D_{t-1} + \sigma_d \epsilon_t^d.$$
$$\ln Z_t = \rho_z \ln Z_{t-1} + \sigma_z \epsilon_t^z.$$
$$m_t = \sigma_m \epsilon_t^m.$$

Both the discount factor D_t and TFP Z_t are assumed to be AR(1) in logs, while the monetary shock m_t is assumed to be serially uncorrelated. A minimum state variable representation of the model has five states $\mathbb{S}_t = \{N_{t-1}, Z_t, m_t, Z_{t-1}, D_t\}$ and three policies $\{\Pi(\mathbb{S}_t), \omega(\mathbb{S}_t), \theta(\mathbb{S}_t)\}$. The equilibrium conditions are summarized in Appendix E

6 Empirical Evidence

Building on the theoretical framework established in the previous section, which analytically demonstrates that in a New Keynesian model with labor market frictions, the transmission of monetary policy shocks depends on the surplus of the firm, this section presents empirical evidence that aligns with this theory. We show robustness by looking at two different methodologies, three different proxies for surplus, and three different monetary policy shock instruments.

6.1 Empirical Framework

State-Dependent Local Projections Following Cloyne, Jordà, and Taylor (2023), one can extend the standard Local Projection (Jordà, 2005) framework to allow for state-dependent impulse responses. Specifically, consider a *state variable* x_t. The state-dependent local projection framework is given by:

$$y_{t+h} = \alpha_h + \beta_h s_t + \beta_h^x s_t (x_t - \bar{x}) + w_t \gamma_h + \varepsilon_t, \quad \text{for } h = 0, \ldots, H \text{ and } t = 1, \ldots, T, \tag{22}$$

where w_t is a set of control variables, augmented with $(x_t - \bar{x})$, representing deviations of the state variable from its steady-state level $\bar{x}$. Relative to a standard Local Projection, the state-dependent specification introduces the term $\beta_h^x s_t (x_t - \bar{x})$, which captures the interaction between the shock s_t and the state variable x_t. The state-dependent impulse response function is then given by the sum of the direct effect of the shock, $\hat{\beta}_h$, and the state-dependent effect, $\hat{\beta}_h^x (x_t - \bar{x})$.[13] We use an instrumental variable (IV) approach,

[13]To aid inference, we impose the restriction that the response for each month in a quarter is the same, reducing the number of parameters to be estimated and shortening confidence intervals.

where the shock s_t is replaced by a policy variable, such as the Federal Funds Rate (FFR), instrumented in a first stage using an exogenous shock series. Given the model includes an interaction term, the instrument set is extended by the interaction between the exogenous shock and the deviation of the state variable from its steady-state level.

Smooth Transition Local Projections A second way to incorporate state dependence in local projections is through the smooth transition local projection (STLP) approach, as in Tenreyro and Thwaites (2016). This approach allows for nonlinear state dependence by modeling the transition between regimes as a smooth function of the underlying state variable. This is achieved by augmenting the local projections framework with a transition function $g(x_t)$, which smoothly varies between 0 and 1 depending on the state variable x_t. The STLP specification can be written as:

$$y_{t+h} = (\alpha_h + \beta_h s_t + w_t \gamma_h)\big[1 - g(x_t)\big] + (\alpha_h^g + \beta_h^g s_t + w_t \gamma_h^g) g(x_t) + \varepsilon_t. \tag{23}$$

A common choice for the transition function is the logistic function $g(x_t) = [1+\exp(-\theta(x_t - c))]^{-1}$, where θ determines the speed of transition between regimes and c is the threshold level of the state variable. The coefficients β_h and β_h^g capture the responses of y_{t+h} to the shock s_t in the low and high regimes, respectively. The IRF at any point in time is given by a weighted average of these responses, with the weights determined by $g(x_t)$.

6.2 Data Description

Outcome Variables The empirical analysis focuses on the effects of monetary policy shocks on the following real-side variables: the Industrial Production Index (IPI), the unemployment rate, vacancies (from the Job Openings and Labor Turnover Survey, and measured using the Help-Wanted Index from Barnichon (2010) before December 2001), and market tightness (the ratio of vacancies to unemployment). In addition to these real-side variables, we consider two price variables: the Consumer Price Index (CPI) and real wages, where real wages are calculated as the log of average hourly earnings divided by the CPI. Detailed descriptions of the data sources and transformations are provided in Appendix A.

Controls In the local projection instrumental variable framework, we follow the approach of Ramey (2016) by including controls for the CPI, the unemployment rate, the Producer Price Index (PPI), and lags of the monetary policy variable and the dependent variable. Following the recommendations of Bauer and Swanson (2023), the LP-IV framework

includes 12 monthly lags. For the STLP analysis, we adopt the same controls, number of lags, time period, and specifications as in Tenreyro and Thwaites (2016).

State Variables The empirical analysis in this section uses three proxies of firm surplus as were motivated in the previous section to examine state-dependent monetary policy transmission:

1. Corporate Profits: Corporate profits are measured as the ratio of profits to the sum of profits and compensation, as reported in the National Income and Product Accounts (NIPA), Table 1.10.
2. Marginal Cost of Hiring: Marginal hiring costs in our model scale with the log of market tightness minus the log of the job finding rate. For the job finding rate, we follow Shimer (2005).
3. Total Factor Productivity (TFP): We use the quarterly TFP growth proxy constructed by Fernald (2014). From this measure, we create a TFP index, which is detrended using the Hamilton (2018) filter to obtain a proxy for TFP levels.

We acknowledge that a causal interpretation of this framework relies on the exogeneity of the monetary policy shocks with respect to both state and outcome variables at all horizons (Gonçalves, Herrera, Kilian, and Pesavento, 2023) — a condition that may not be satisfied. Our aim in this section is more modest: to document correlations indicative of state dependence that are consistent with the theoretical model.

Instruments and Policy Variables For the LP-IV framework, we employ three commonly used instruments:

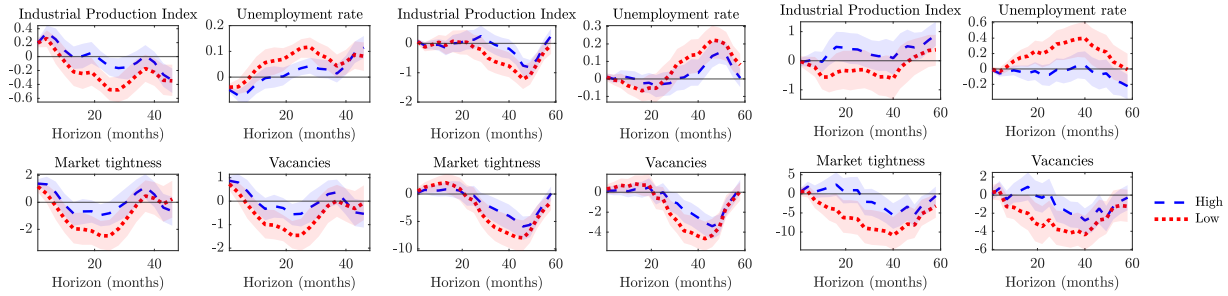
1. The monetary policy shocks from Romer and Romer (2004), extended by Wieland and Yang (2020) to 2007, used to instrument the Federal Funds Rate (FFR).
2. The high-frequency identification approach of Bauer and Swanson (2023), starting in 1989, and we use the data up until 2019, used to instrument the two-year U.S. Treasury yield.
3. The language-processing approach of Aruoba and Drechsel (2024), spanning 1982-2008, used to instrument the two-year U.S. Treasury yield.

In the STLP framework, we follow Tenreyro and Thwaites (2016) and use the extended Romer and Romer (2004) series as the identified monetary policy instrument.

6.3 Empirical evidence on surplus-dependence

Figure 8: State-Dependent Local Projections (State Proxy: Corporate Profits), with the state ± 1 standard deviation above and below the mean

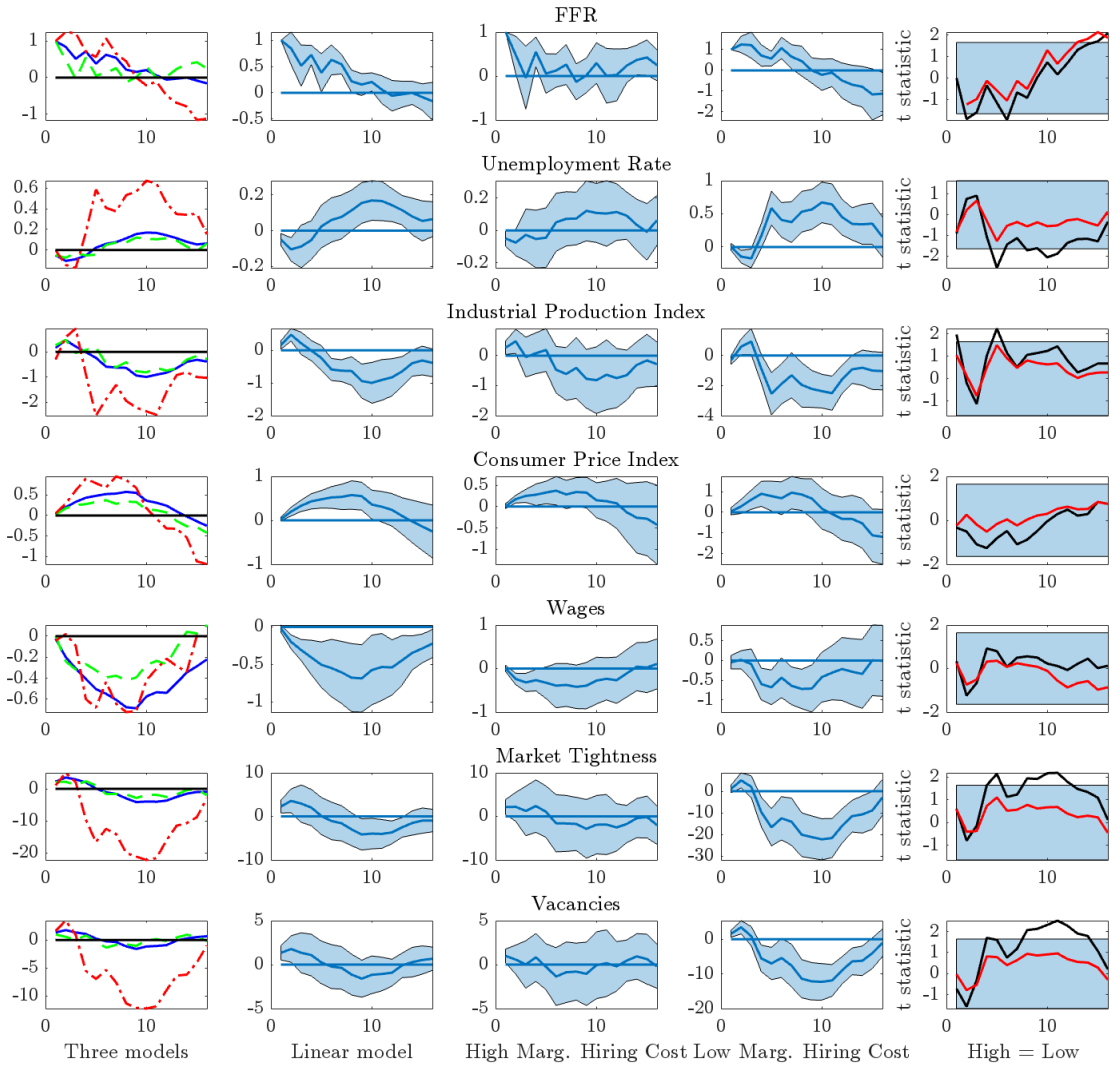
(a) Romer and Romer (2004) shocks as instrument *(b) Aruoba and Drechsel (2024) shocks as instrument* *(c) Bauer and Swanson (2023) shocks as instrument*



Quantities We focus on the state-dependent effects on quantities: the unemployment rate, IPI, vacancies, and market tightness. Figure 8 visualizes the implied impulse response functions in a low profit (one standard deviation below the mean) and high profit (one std. above the mean) state, based on the corporate profit proxy. The FFR in case of Romer and Romer (2004), and the two-year Treasury yield for the other shocks, are instrumented using the monetary policy shocks identified by Romer and Romer (2004), Aruoba and Drechsel (2024) and Bauer and Swanson (2023), respectively. The figure shows the estimated effects on real variables are broadly consistent across all three instruments, confirming our theory that in times of low profit, the real effects of monetary policy shocks are larger. Appendix Section B shows that similar results can be found for the other proxies. We also find similar results using the smooth transition local projection, presented in Figure 9 for the marginal hiring cost proxy, and in Appendix Figures B3 and B4 for the other two proxies.

Prices and Wages The results regarding state dependence in price variables are more ambiguous, with different methodologies yielding inconsistent signs. However, it is well recognized that in local projections, price responses can be affected by the so-called price puzzle (see, e.g., the discussion in Ramey (2016)). Therefore, we do not emphasize the sign of state dependence but rather focus on its magnitude. As shown in Appendix section B, the differences in inflation and wage responses between high- and low-surplus states are not economically meaningful.

Figure 9: Smooth Transition Local Projections Using Marginal Hiring Costs as a Proxy for Surplus



Note: The first four columns show the response of the outcome variable to a 1 percentage point change in the FFR on impact across 16 horizons (quarters). In the first column, the average response (solid), the high-surplus (dashed) and the low-surplus (dash-dot) are shown on the same axis. The next three columns show the average response, high-surplus and low-surplus response respectively, with 90% confidence intervals. The last column tests the hypothesis that the coefficients in the high and low surplus regime are equal, where the red line is computed using a Bootstrap, and the black line using the Driscoll-Kraay method, and shaded area is ± 1.65. For details we refer to Tenreyro and Thwaites (2016).

Comparison with results in Tenreyro and Thwaites (2016) Tenreyro and Thwaites (2016) find that monetary policy has larger effects during expansions than during recessions. At first glance, this may seem to contradict our findings, as one may think that expansions are high surplus periods, and our results instead suggest that monetary policy has smaller real-side effects when surplus is high. In Appendix Section C, we provide a discussion on

how the state used in Tenreyro and Thwaites (2016) is negatively correlated to our surplus proxies.

7 Model Results

We now present results from our quantitative model, solved using Taylor projections and using the Time-Varying Kalman Filter to infer the underlying states of the economy. This approach enables us to compute implied impulse response functions over time, as well as other objects of interest to policymakers, and to quantify the extent of state dependence in the U.S. economy.

The data used for estimation are summarized in Table A2 in the Appendix. This table also details the data transformations applied. Our three key variables of interest are market tightness, the federal funds rate, and inflation. We analyze data spanning the period from 1967 to 2019 at a quarterly frequency for estimation, and 1967-2024 for filtering after estimation.

7.1 Parameter Estimates

A subset of parameters are calibrated, which are described and provided in Table 3. Priors and posteriors are described in Table 4, comparing both linear and nolinear parameter estimates. Linear and nonlinear parameters vary substantially, which is not surprising given the large nonlinearities in the model. Note that the linear model is estimated on a sample up to 2007 because of the ZLB, which may further contribute to the differences between sestimates.

7.2 External validation: assessing our state proxies

After filtering the states, we compute the surplus proxies implied by our model and compare them with the proxies used in the empirical section. This serves as an external validity check. As shown in Figure 10 all three model-implied proxies are positively correlated with the data proxies, none of which are directly used to estimate the model. This suggests the empirical evidence used to motivate the quantitative model is broadly consistent with the model implied states.

Table 3: Calibrated parameters

Parameter	Calibrated value
α: matching function	0.8
τ: risk aversion	1
h: habits	0.1
ψ_π: inflation weight in Taylor Rule	2
ψ_y: output weight in Taylor Rule	0.2
Π_{ss}: steady state inflation	1.005
R_{ss}: steady state interest rate	1.015
q_{ss}: steady state vacancy-filling rate	0.7
θ_{ss}: steady state market tightness	1
n_{ss}: steady state employment	0.94
δ: exogenous job destruction rate	$\frac{q_{ss}\theta_{ss}(1-n_{ss})}{(1-q_{ss}\theta_{ss})n_{ss}}$
s_{ss}: steady state separation rate	$\log \delta$
a_{ss}: steady state match efficiency	$\log \frac{q_{ss}}{(1+\theta_{ss}^{\alpha})^{-1/\alpha}}$
κ: vacancy cost	$\frac{(1-\eta)(1-\gamma-b)q_{ss}}{1-\beta(1-\delta)}$

7.3 Phillips Multiplier

A key concern for policymakers is the unemployment-inflation trade-off, which captures the nominal effects relative to the real effects of a monetary shock. However, state dependence in impulse responses alone does not necessarily imply variation in the unemployment-inflation trade-off; this depends on whether the real versus nominal effects differ in relative magnitude across states. To illustrate that the unemployment-inflation trade-off is state dependent, we use the concept of the Phillips multiplier, as in Barnichon and Mesters (2021), motivated by Mankiw (2001). The Phillips multiplier quantifies this trade-off by measuring the average change in inflation caused by an interest rate change that reduces the unemployment rate by one percentage point over h periods:

$$T_h = \frac{\partial \bar{\Pi}_{t:t+h}}{\partial R_t}\Big|_{\varepsilon_t} \Big/ \frac{\partial \bar{U}_{t:t+h}}{\partial R_t}\Big|_{\varepsilon_t}$$

Here $\bar{\Pi}_{t:t+h}$ is the average over variable Π over h time periods, and ε_t is the exogenous change in the interest rates. The statistical counterpart of T_h is the so-called Phillips multiplier (Barnichon and Mesters, 2021):

$$\mathcal{P}_h = \mathcal{R}_h^{\bar{\Pi}} / \mathcal{R}_h^{\bar{U}}, \quad h = 0, 1, 2, ...,$$

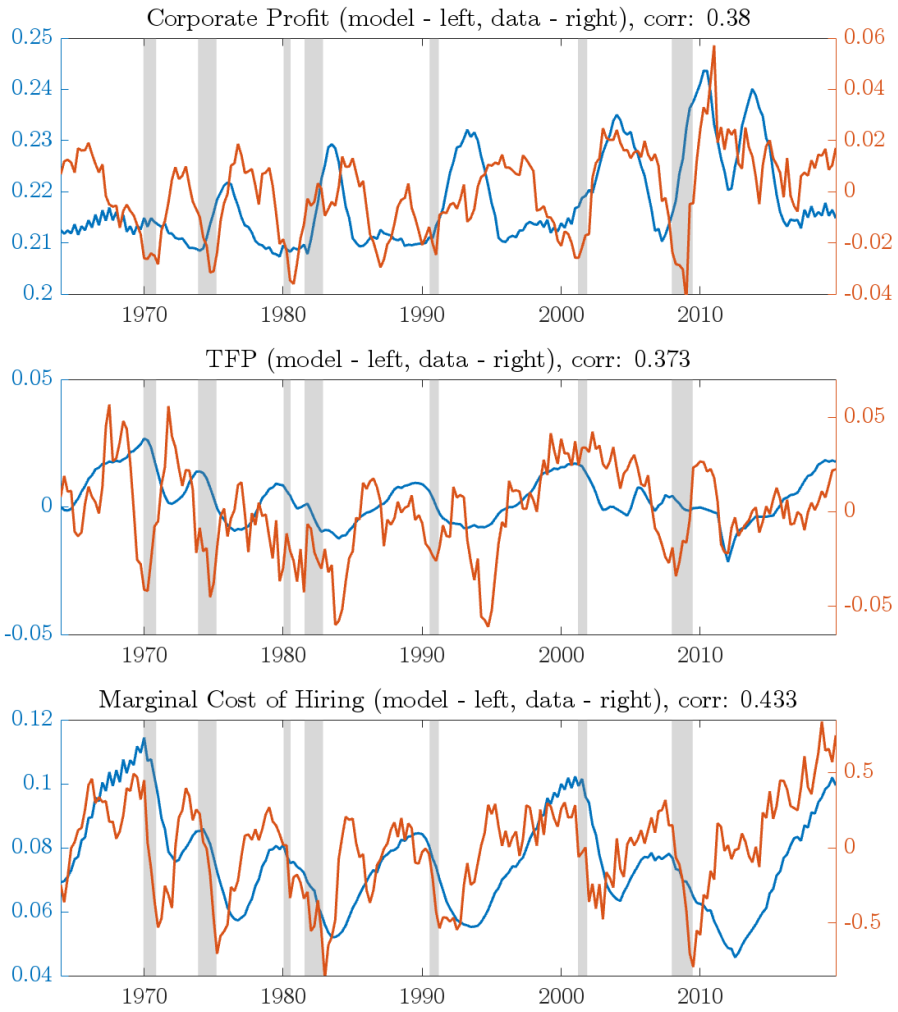
Table 4: Prior distribution with mean and standard deviation, posterior means and standard deviations for log-linear and TP-KF (based on 20,000 draws, acceptance rate of 36%, burn-in 5,000, thin 3).

Parameter	Prior	Posterior			
		Log-linear		TP-KF	
	Distr.(Mean, Std.)	Mean	Std.	Mean	Std.
ϕ: price adjustment cost	Gamma(12.5, 2)	20.133	1.212	19.53	0.639
ν: flow value unemployment	Beta(0.87, 0.005)	0.867	0.002	0.892	3e-4
η: bargaining weight	Beta(0.5, 0.25)	0.884	0.066	0.623	0.015
ρ_r: inertia Taylor rule	Beta(0.1, 0.05)	0.142	0.012	0.318	0.009
ρ_z: persistence TFP	Beta(0.5, 0.1)	0.868	0.009	0.641	0.010
ρ_d: persistence DF	Beta(0.5, 0.1)	0.902	0.017	0.815	0.014
ρ_s: persistence separations	Beta(0.5, 0.1)	0.672	0.031	0.502	0.022
ρ_a: persistence matching efficiency	Beta(0.5, 0.1)	0.896	0.035	0.198	0.029
σ_m: std. MP shocks	Gamma(0.05, 5)	0.005	3e-4	0.004	2e-4
σ_z: std. TFP shocks	Gamma(0.05, 5)	0.003	3e-4	0.002	1e-4
σ_d: std. DF shocks	Gamma(0.05, 5)	0.013	0.002	0.010	4e-4
σ_s: std. separation shocks	Gamma(0.05, 5)	0.100	0.006	0.126	0.004
σ_a: std. matching efficiency shocks	Gamma(0.05, 5)	0.008	5e-4	0.007	3e-4
σ_{TG}^{ME}: std. ME tightness	Gamma(0.001, 0.01)	8e-4	4e-4	0.009	0.003
σ_{R}^{ME}: std. ME interest rate	Gamma(0.001, 0.01)	4e-4	1e-4	0.007	3e-4
σ_{Π}^{ME}: std. ME inflation	Gamma(0.001, 0.01)	4e-4	1e-4	9e-4	1e-4
σ_{N}^{ME}: std. ME employment	Gamma(0.001, 0.01)	3e-4	1e-4	0.008	3e-4
σ_{S}^{ME}: std. ME separations	Gamma(0.001, 0.01)	7e-4	4e-4	0.015	0.004

that is, the ratio of the cumulative impulse response function (up to horizon h) of inflation over unemployment. The Phillips Multiplier can loosely be interpreted as the slope of the Phillips curve. In the case of state-dependent impulse response functions, the Phillips Multiplier is also state-dependent when the magnitude of the effect of a monetary shock on inflation relative to unemployment depends on the state of the economy.

Using the model to filter the latent states – employment, TFP, discount factor shock, monetary shock, and lagged TFP – we compute the implied impulse response of a 40 basis point monetary policy shock at each point in time. These impulse responses, evaluated at each filtered state, allow us to compute the Phillips Multiplier over a six-year horizon, after which the cumulative impulse responses stabilize as the effects dissipate. We visualize this filtered series in Figure 11. As shown, the Phillips Multiplier is generally countercyclical, tending to rise during recessions. Several periods stand out where the Phillips curve was particularly flat, typically following a recession. Note, the Phillips Multiplier can be loosely interpreted as the slope of the Phillips curve. One period of particular interest is

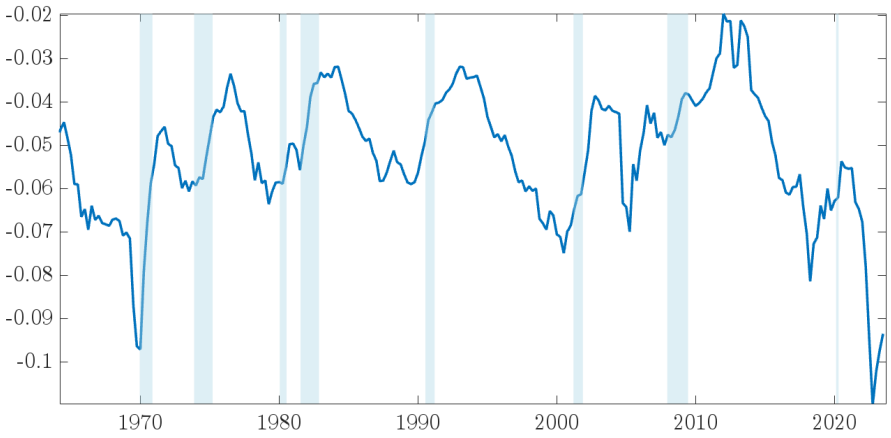
Figure 10: Proxies for Surplus in Data and Through the Lens of the Model



the post-2010 era when the zero lower bound (ZLB) was binding. Conversely, two periods where the Phillips curve was particularly steep occurred around 1970 and 2022. More recently, we observe a steepening trend in the Phillips curve following the departure from the ZLB in the latter part of the sample.

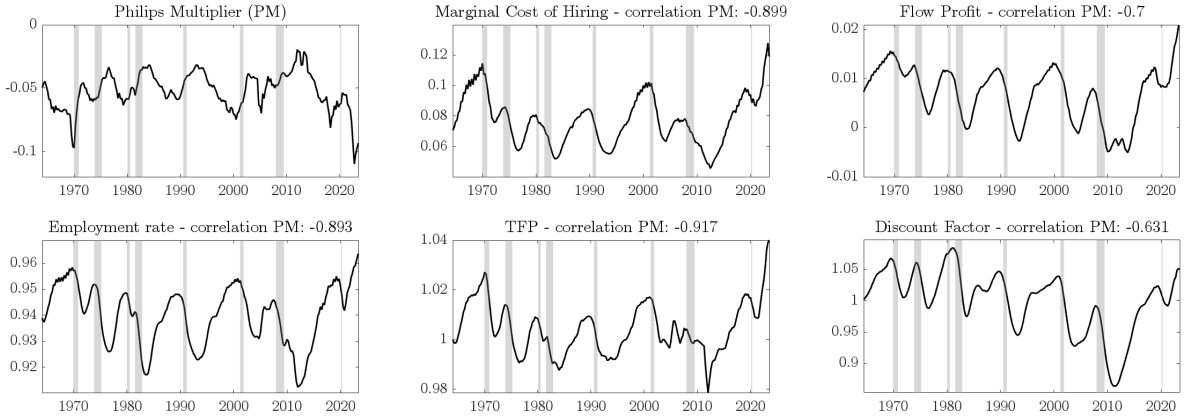
The fluctuations in the Phillips Multiplier can be explained and interpreted through the mechanisms outlined in this paper. To illustrate this, Figure 12 visualizes the Phillips Multiplier alongside relevant proxies and state variables, with their respective correlations noted. For example, the correlation between the model-implied marginal cost of hiring and the Phillips Multiplier across filtered states is -0.899, while its correlation with TFP is

Figure 11: Phillips Multiplier (Filtered)



-0.917. Flow profit exhibits a slightly lower correlation of -0.7 with the Phillips Multiplier, as this are also strongly influenced by the discount factor in this model in the latter part of the sample.

Figure 12: Phillips Multiplier alongside Surplus Proxies and Model States



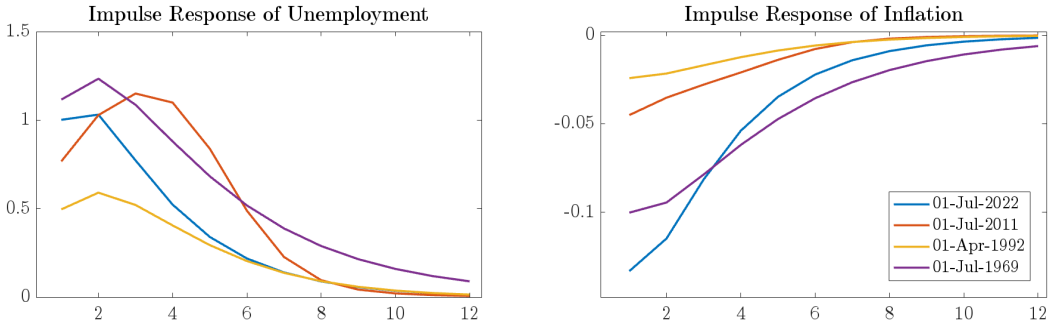
Comparison with other empirical evidence on the Phillips Multiplier Looking at the existing literature, our Phillips Multiplier estimates are consistent with Barnichon and Mesters (2021) post-1990's estimate, and the estimates of Hazell et al. (2022). The range of our estimates is comparable to Gitti (2024), who posits that the Phillips curve is nonlinear in market tightness,[14] and finds a multiplier of -0.03 when markets are slack, versus -0.08 when markets are tight.

[14]By assuming there is a kink in the Phillips curve at market tightness $\theta = 1$

7.4 Time-Varying Impulse Responses

To provide further insights into the state-dependent effects of monetary policy, Figure 13 visualizes impulse response functions for unemployment and inflation at four different points in time, computed based on our filtered states. We consider two periods with a flat Phillips curve, as indicated by our Phillips Multiplier estimates in Figure 11: the zero lower bound (ZLB) period (2011Q3) and 1992Q2. Additionally, we examine two periods with a steep Phillips curve, 2022Q3 and 1969Q3.

Figure 13: Impulse Response Functions over Time



During the two visualized periods of low absolute Phillips Multiplier (PM) values, 2011Q3 and 1992Q2, the inflation response is small. However, the unemployment rate responses differ significantly due to the lower model-implied TFP in 2011Q3, which leads to a larger response compared to 1992Q2, when TFP was near its steady-state value. Conversely, in periods with high absolute PM values, such as 2022Q3 and 1969Q3, we find that the effects of a monetary policy shock on prices are twice as large as in low-PM states, while the cumulative effect on unemployment falls between the values observed in low-PM states. Overall, we conclude that the presence of nonlinearities introduced by labor search frictions leads to significant time variation in the unemployment-inflation trade-off. This variation is driven by both time-varying responses of unemployment and time-varying responses of prices.

8 Conclusion

This paper proposes a new methodology for the estimation of DSGE models featuring various nonlinearities, including state dependence. We build on recent advances in the computational macroeconomic literature, which have developed local linear solution methods to macroeconomic models, as in Fernández-Villaverde and Levintal (2018); Levintal (2018); Mennuni et al. (2024). Local linear solution methods imply a mapping into

a time-varying linear state space model, for which we can use the time-varying Kalman filter to evaluate its likelihood and filter its underlying states. This method is both fast and accurate, and outperforms the particle filter in simulations in both dimensions.

The paper uses the Diamond-Mortensen-Pissarides model to explain and demonstrate the method, where the model is chosen for its known strong nonlinearities (Petrosky-Nadeau and Zhang, 2017). We then also illustrate the method in the textbook New Keynesian model, showing that when solved and estimated nonlinearly, the model can rationalize a mild flattening of the Phillips curve between the 80s and 00s, driven by a declining discount factor over that period.

Next, in our main application, the paper establishes a link between time variation in the effects of monetary policy due to search frictions in the labor market. We first demonstrate this analytically in a stylized New Keynesian model with labor market frictions, motivating empirical proxies for flow surplus - the key determinate of state-dependent propagation in this class of models. Using these proxies, we provide model-free evidence that monetary policy shocks have stronger real effects when flow profit is low. To further explore this mechanism, we develop a quantitative model, and use our estimation procedure to recover time-varying impulse response functions and Phillips Multipliers, revealing substantial variation in monetary policy effectiveness over the business cycle. Notably, we find that the Phillips Multiplier is twice as small during recessions as it is during expansions.

State dependence in the effects of monetary policy and the slope of the Phillips curve are critical considerations for policymakers. Our framework allows them to filter the underlying state of the economy and compute the implied impulse response functions and Phillips Multiplier in real time, ensuring that policy decisions are informed by current economic conditions rather than historical averages. More broadly, our modeling and filtering approach offers a generalizable framework for analyzing time-varying macroeconomic relationships. This methodology can be extended to study other forms of state dependence in policy transmission.

References

Adjemian, S., Juillard, M., Karamé, F., Mutschler, W., Pfeifer, J., Ratto, M., ... Villemot, S. (2024). *Dynare: Reference manual, version 6* (Dynare Working Papers No. 80). CEPREMAP.

Ahn, H. J., and Hamilton, J. D. (2022). "Measuring labor-force participation and the incidence and duration of unemployment". *Review of Economic Dynamics*, *44*, 1-32.

Amisano, G., and Tristani, O. (2010). "Euro Area Inflation Persistence in an Estimated Nonlinear DSGE Model". *Journal of Economic Dynamics and Control*, *34*(10), 1837–1858.

An, S., and Schorfheide, F. (2007). "Bayesian Analysis of DSGE Models". *Econometric reviews*, *26*(2-4), 113–172.

Aruoba, S. B., Cuba-Borda, P., and Schorfheide, F. (2018). "Macroeconomic Dynamics near the ZLB: A Tale of Two Countries". *The Review of Economic Studies*, *85*(1), 87–118.

Aruoba, S. B., and Drechsel, T. (2024). *"Identifying Monetary Policy Shocks: A Natural Language Approach"* (Tech. Rep.). National Bureau of Economic Research.

Barnichon, R. (2010). "Building a Composite Help-Wanted Index". *Economics Letters*, *109*(3), 175–178.

Barnichon, R., and Mesters, G. (2021). "The Phillips Multiplier". *Journal of Monetary Economics*, *117*, 689–705.

Bauer, M. D., and Swanson, E. T. (2023). "A Reassessment of Monetary Policy Surprises and High-Frequency Identification". *NBER Macroeconomics Annual*, *37*(1), 87–155.

Benigno, P., and Eggertsson, G. B. (2023). *"It's baaack: The Surge in Inflation in the 2020s and The return of the Non-Linear Phillips Curve"* (Tech. Rep.). National Bureau of Economic Research.

Benigno, P., and Eggertsson, G. B. (2024). "Slanted-L Phillips Curve". In *Aea papers and proceedings* (Vol. 114, pp. 84–89).

Berentsen, A., Menzio, G., and Wright, R. (2011). Inflation and unemployment in the long run. *American Economic Review*, *101*(1), 371–398.

Blanchard, O., and Galí, J. (2010). "Labor markets and monetary policy: A new keynesian model with unemployment". *American economic journal: macroeconomics*, *2*(2), 1–30.

Christiano, L. J., Eichenbaum, M., and Trabandt, M. (2016). "Unemployment and Business Cycles". *Econometrica*, *84*(4), 1523–1569.

Cloyne, J., Jordà, Ò., and Taylor, A. M. (2023). *"State-Dependent Local Projections: Understanding Impulse Response Heterogeneity"* (Tech. Rep.). National Bureau of Economic Research.

Coibion, O., and Gorodnichenko, Y. (2015). "Is the Phillips Curve Alive and Well After All? Inflation Expectations and the Missing Disinflation". *American Economic Journal: Macroeconomics*, *7*(1), 197–232.

Diamond, P. A. (1982). "Wage Determination and Efficiency in Search Equilibrium". *The Review of Economic Studies*, *49*(2), 217–227.

Dotsey, M., King, R. G., and Wolman, A. L. (1999). "State-Dependent Pricing and the General Equilibrium Dynamics of Money and Output". *The Quarterly Journal of Economics*, *114*(2), 655–690.

Durbin, J., and Koopman, S. J. (2012). *"Time Series Analysis by State Space Methods"* (Vol. 38). OUP Oxford.

Eichenbaum, M., Puglisi, F., Rebelo, S., and Trabandt, M. (2025). *"Banks and the State-Dependent Effects of Monetary Policy"* (Tech. Rep.). National Bureau of Economic Research.

Eichenbaum, M., Rebelo, S., and Wong, A. (2022). "State-dependent Effects of Monetary Policy: The Refinancing Channel". *American Economic Review*, *112*(3), 721–761.

Farmer, L. E. (2021). "The Discretization Filter: A Simple Way to Estimate Nonlinear State Space Models". *Quantitative Economics*, *12*(1), 41–76.

Fernald, J. (2014). "A Quarterly, Utilization-Adjusted Series on Total Factor Productivity"..

Fernández-Villaverde, J., and Levintal, O. (2018). "Solution Methods for Models with Rare Disasters". *Quantitative Economics*, *9*(2), 903–944. Retrieved from https://www.sas.upenn.edu/~jesusfv/rare_disasters.pdf doi: 10.3982/QE895

Fernández-Villaverde, J., and Rubio-Ramírez, J. F. (2005). "Estimating Dynamic Equilibrium Economies: Linear versus Nonlinear Likelihood". *Journal of Applied Econometrics*, *20*(7), 891–910.

Fernández-Villaverde, J., and Rubio-Ramírez, J. F. (2007). "Estimating Macroeconomic Models: A Likelihood Approach". *The Review of Economic Studies*, *74*(4), 1059–1087.

Gali, J. (2015). *"Monetary Policy, Inflation, and the Business Cycle: An Introduction to the New Keynesian Framework and Its Applications"* (2nd ed.). Princeton University Press.

Galí, J., Smets, F., and Wouters, R. (2012). "Unemployment in an estimated New Keynesian model". *NBER macroeconomics annual*, *26*(1), 329–360.

Gertler, M., and Leahy, J. (2008). "A Phillips Curve with an Ss Foundation". *Journal of Political Economy*, *116*(3), 533–572.

Gertler, M., Sala, L., and Trigari, A. (2008). "An Estimated Monetary DSGE Model with Unemployment and Staggered Nominal Wage Bargaining'. *Journal of Money, Credit and Banking*, *40*(8), 1713–1764.

Gitti, G. (2024). *"Nonlinearities in the Regional Phillips Curve with Labor Market Tightness"*. unpublished manuscript, Brown University.

Gonçalves, S., Herrera, A. M., Kilian, L., and Pesavento, E. (2023). "State-Dependent Local Projections".

Gust, C., Herbst, E., López-Salido, D., and Smith, M. E. (2017). "The Empirical Implications of the Interest-rate Lower Bound". *American Economic Review*, *107*(7), 1971–2006.

Hamilton, J. D. (1994). *"Time Series Analysis"*. Princeton University Press.

Hamilton, J. D. (2018). "Why You Should Never Use the Hodrick-Prescott Filter". *Review of Economics and Statistics*, *100*(5), 831–843.

Harding, M., Lindé, J., and Trabandt, M. (2022). "Resolving the Missing Deflation Puzzle". *Journal of Monetary Economics*, *126*, 15–34.

Harding, M., Lindé, J., and Trabandt, M. (2023). "Understanding Post-Covid Inflation Dynamics". *Journal of Monetary Economics*.

Hazell, J., Herreno, J., Nakamura, E., and Steinsson, J. (2022). "The Slope of the Phillips Curve: Evidence from US States". *The Quarterly Journal of Economics*, *137*(3), 1299–1344.

Herbst, E. P., and Schorfheide, F. (2016). *"Bayesian Estimation of DSGE Models"*. Princeton University Press.

Jordà, Ò. (2005). "Estimation and Inference of Impulse Responses by Local Projections". *American Economic Review*, *95*(1), 161–182.

Judd, K. L., Maliar, L., and Maliar, S. (2017). "Lower Bounds on Approximation Errors to Numerical Solutions of Dynamic Economic Models". *Econometrica*, *85*(3), 991–1012.

Krause, M. U., Lopez-Salido, D., and Lubik, T. A. (2008). "Inflation Dynamics with Search Frictions: A Structural Econometric Analysis". *Journal of Monetary Economics*, *55*(5), 892–916.

Krause, M. U., and Lubik, T. A. (2007). "The (ir) relevance of real wage rigidity in the New Keynesian model with search frictions". *Journal of Monetary Economics*, *54*(3), 706–727.

Lahcen, M. A., Baughman, G., Rabinovich, S., and van Buggenum, H. (2022). "Nonlinear Unemployment Effects of the Inflation Tax". *European Economic Review*, *148*, 104247.

Levintal, O. (2018). "Taylor Projection: A New Solution Method for Dynamic General Equilibrium Models". *International Economic Review*, *59*(3), 1345–1373. Retrieved from https://doi.org/10.1111/iere.12306 doi: 10.1111/iere.12306

Mankiw, N. G. (2001). "The Inexorable and Mysterious Tradeoff Between Inflation and Unemployment". *The Economic Journal*, *111*(471), 45–61.

Mennuni, A., Rubio-Ramírez, J. F., and Stepanchuk, S. (2024, April). "Dynamic Perturbation". *The Review of Economic Studies*. Retrieved from https://academic.oup.com/restud/advance-article/doi/10.1093/restud/rdae037 (Advance online publication) doi: 10.1093/restud/rdae037

Mortensen, D. T. (1982). "Property Rights and Efficiency in Mating, Racing, and Related Games". *The American Economic Review*, *72*(5), 968–979.

Petrosky-Nadeau, N., and Zhang, L. (2017). "Solving the Diamond–Mortensen–Pissarides Model Accurately". *Quantitative Economics*, *8*(2), 611–650.

Phillips, A. W. (1958). "The Relation between Unemployment and the Rate of Change of Money Wage Rates in the United Kingdom, 1861-1957". *Economica*, *25*(100), 283–299.

Pissarides, C. A. (1985). "Short-run Equilibrium Dynamics of Unemployment, Vacancies, and Real Wages". *American Economic Review*, *75*(4), 676–690.

Ramey, V. A. (2016). "Macroeconomic Shocks and Their Propagation". *Handbook of Macroeconomics*, *2*, 71–162.

Romer, C. D., and Romer, D. H. (2004). "A New Measure of Monetary Shocks: Derivation and Implications". *American Economic Review*, *94*(4), 1055–1084.

Rotemberg, J. J. (1982). "Sticky prices in the United States". *Journal of Political economy*, *90*(6), 1187–1211.

Schmitt-Grohé, S., and Uribe, M. (2004). "Solving Dynamic General Equilibrium Models Using a Second-Order Approximation to the Policy Function". *Journal of Economic Dynamics and Control*, *28*(4), 755–775.

Shimer, R. (2005, March). "The Cyclical Behavior of Equilibrium Unemployment and Vacancies". *American Economic Review*, *95*(1), 25–49. Retrieved from https://www.aeaweb.org/articles?id=10.1257/0002828053828572 doi: 10.1257/0002828053828572

Smith, S., Timmermann, A., and Wright, J. H. (2023). *"Breaks in the Phillips Curve: Evidence from Panel Data"* (Tech. Rep.). National Bureau of Economic Research.

Stock, J. H., and Watson, M. W. (2020). "Slack and Cyclically Sensitive Inflation". *Journal of Money, Credit and Banking*, *52*(S2), 393–428.

Tenreyro, S., and Thwaites, G. (2016). "Pushing on a String: US Monetary Policy is Less Powerful in Recessions". *American Economic Journal: Macroeconomics*, *8*(4), 43–74.

Thomas, C. (2011). "Search frictions, real rigidities, and inflation dynamics". *Journal of Money, Credit and Banking*, *43*(6), 1131–1164.

Wieland, J. F., and Yang, M.-J. (2020). "Financial Dampening". *Journal of Money, Credit and Banking*, *52*(1), 79–113.

Winschel, V., and Krätzig, M. (2010). "Solving, Estimating, and Selecting Nonlinear Dynamic Models without the Curse of Dimensionality". *Econometrica*, *78*(2), 803–821.

Supplementary Appendix to "Unemployment and the State-Dependent Effects of Monetary Policy"

Eva F. Janssens & Sean McCrary

February, 2025

A Data

Table A1: Data details: Outcome Variables, Controls and State Proxies for Local Projections, Obtained January 9th, 2025.

Variable	Details	Transformation	Source
Unemployment Rate	Percent, Monthly, Seasonally Adjusted	None	LNS14000000
Real Wages	Average Hourly Earnings of Production and Nonsupervisory Employees, Total Private, Dollars per Hour, Monthly, Seasonally Adjusted	$100 \times \log(W/CPI)$	CES0500000008
Federal Funds Rate	Percent, Monthly, Not Seasonally Adjusted	None	DFF
Market tightness	Vacancy over unemployments	$100 \times \log$	Barnicon (2010) & FRED
Job finding rate		$100 \times \log$	Shimer (2005)
CPI	Consumer Price Index for All Urban Consumers: All Items in U.S. City Average, Index 1982-1984=100, Monthly, Seasonally Adjusted	$100 \times \log$	CPIAUCSL
PPI	Producer Price Index by Commodity: All Commodities, Index 1982=100, Monthly, Not Seasonally Adjusted	$100 \times \log$	PPIACO
IPI	Industrial Production: Total Index, Index 2017=100, Monthly, Seasonally Adjusted	$100 \times \log$	IP.B50001.S
HWI	Help-Wanted-Index from Barnicon (2010), JOLTS post 2001	$100 \times \log$	Barnicon (2010)
TFP	1 quarter moving average of TFP growth	Made into Index, Log, Hamilton Filter	Fernald (2014)
Corporate Profits	(Profit/Profit+Compensation)	log, Hamilton Filter	NIPA Table 1.10

Table A2: Data details: estimation and filtering

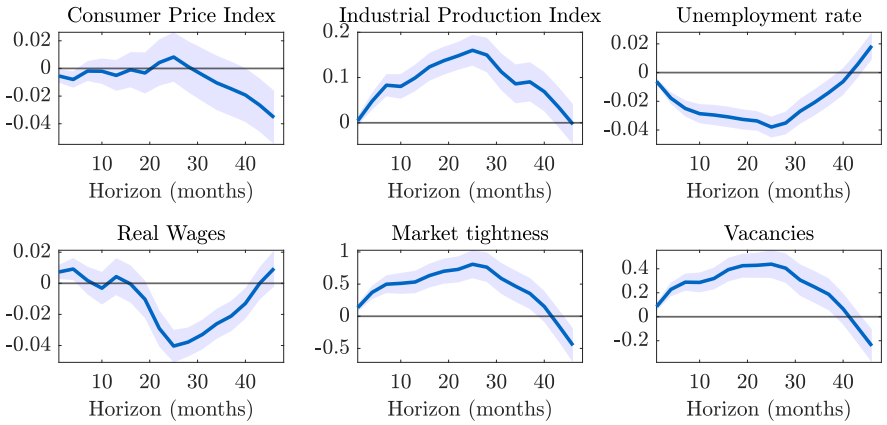
Variable	Details	Transformation	Source
Unemployment Rate	Percent, Quarterly, Seasonally Adjusted	Detrended*	UNRATE (FRED)
Average Weekly Earnings of Production and Nonsupervisory Employees Total Private	Dollars per Week, Quarterly, Seasonally Adjusted	Detrended* & demeaned	CES0500000030 (FRED)
Nonfarm Business Sector: Output per Worker	Index 2017=100 Quarterly Seasonally Adjusted	Detrended* & demeaned	PRS85006163
Market tightness	Vacancy over unemployments	Detrended*	Barnicon (2010) & FRED
Federal Funds Effective Rate	Percent	Quarterly**	DFF
CPI	Consumer Price Index for All Urban Consumers: All Items in U.S. City Average Index 1982-1984=100, Monthly, Seasonally Adjusted	Quarter-to-quarter % ch., detrended*	CPIAUCSL

Notes: (*) We use the Hamilton filter to remove long-run trends (Hamilton, 2018). (**) DFF converted to a quarterly interest rate $(100 * ((1 + DFF/100)^{(1/4)} - 1))$.

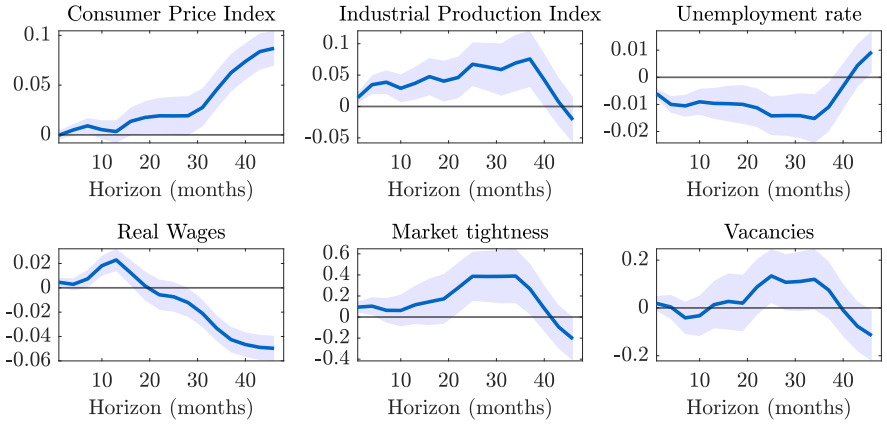
B Additional Results for the Local Projections

Figure B1: Interaction Term of Surplus and Federal Funds Rate (as in Eq. (22)), instrumented using the Romer and Romer (2004) shocks.

(a) Corporate Profits as a surplus proxy



(b) Marginal Cost of Hiring as a surplus proxy



(c) Total Factor Productivity as a surplus proxy

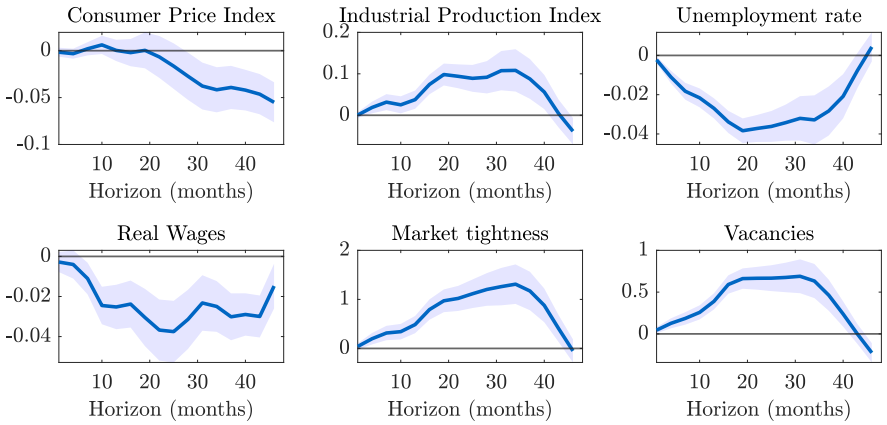
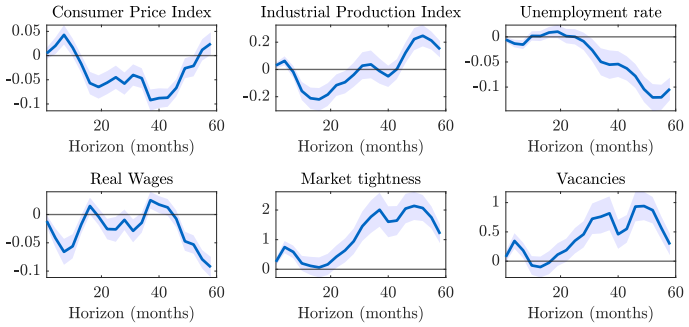
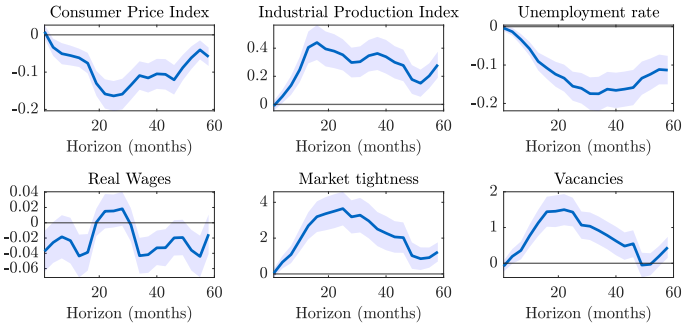


Figure B2: Interaction Term of Surplus Proxy and Policy Variable (as in Eq. (22)).

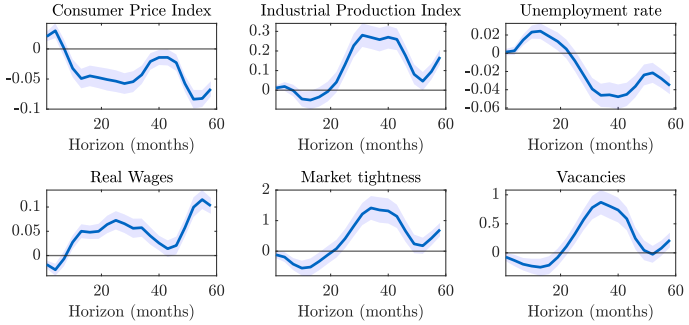
(a) Interaction of Two-Year Treasury Yield and Total Factor Productivity, using the Bauer and Swanson (2023) Instrument



(b) Interaction of Two-Year Treasury Yield and Profit, using the Bauer and Swanson (2023) Instrument



(c) Interaction of Two-Year Treasury Yield and Profit, using the Aruoba and Drechsel (2024) Instrument



(d) Interaction of Two-Year Treasury Yield and Marginal Hiring Cost, using the Aruoba and Drechsel (2024) Instrument

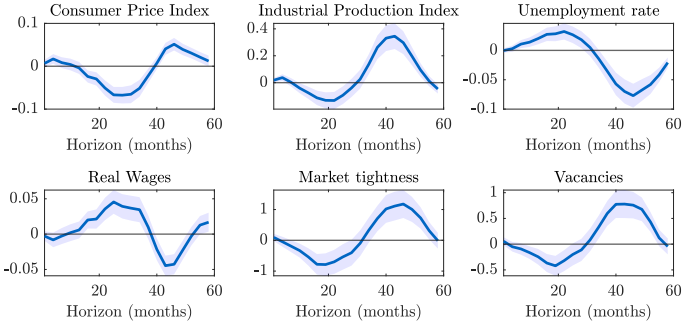
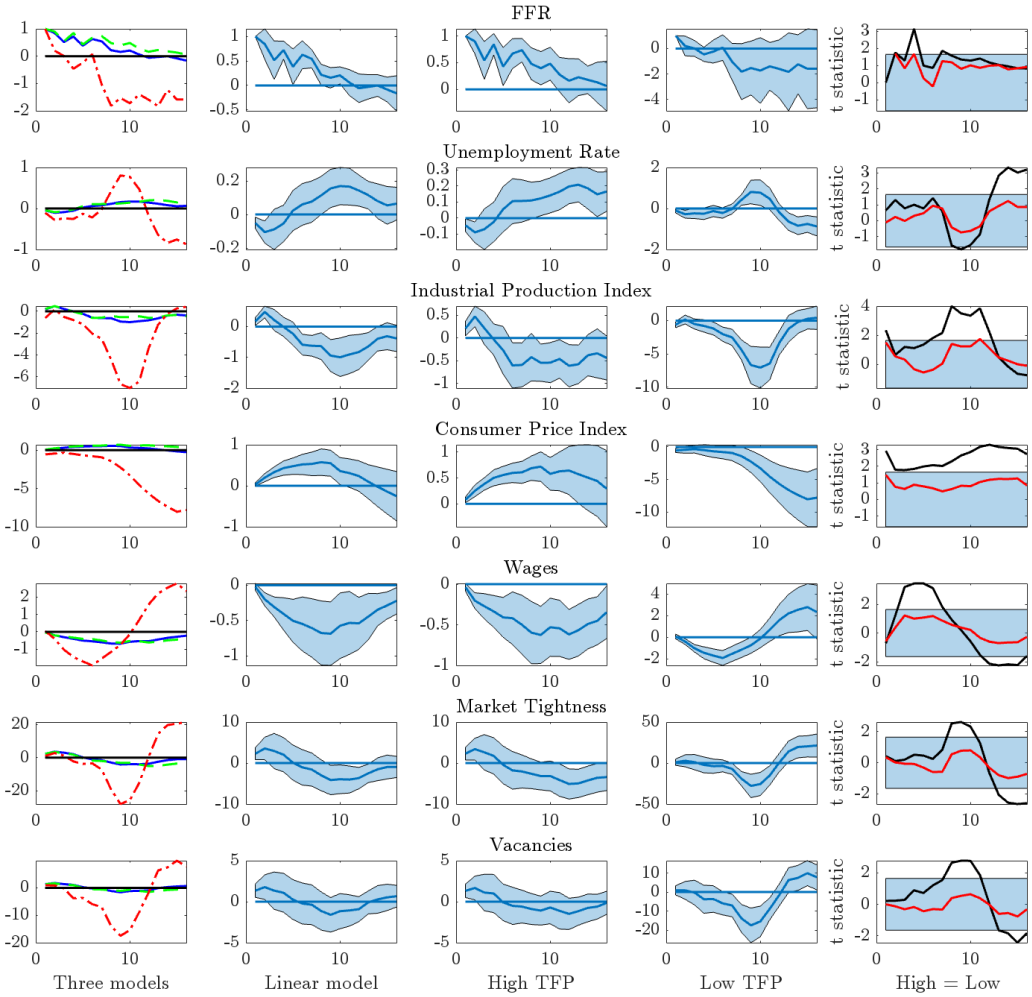
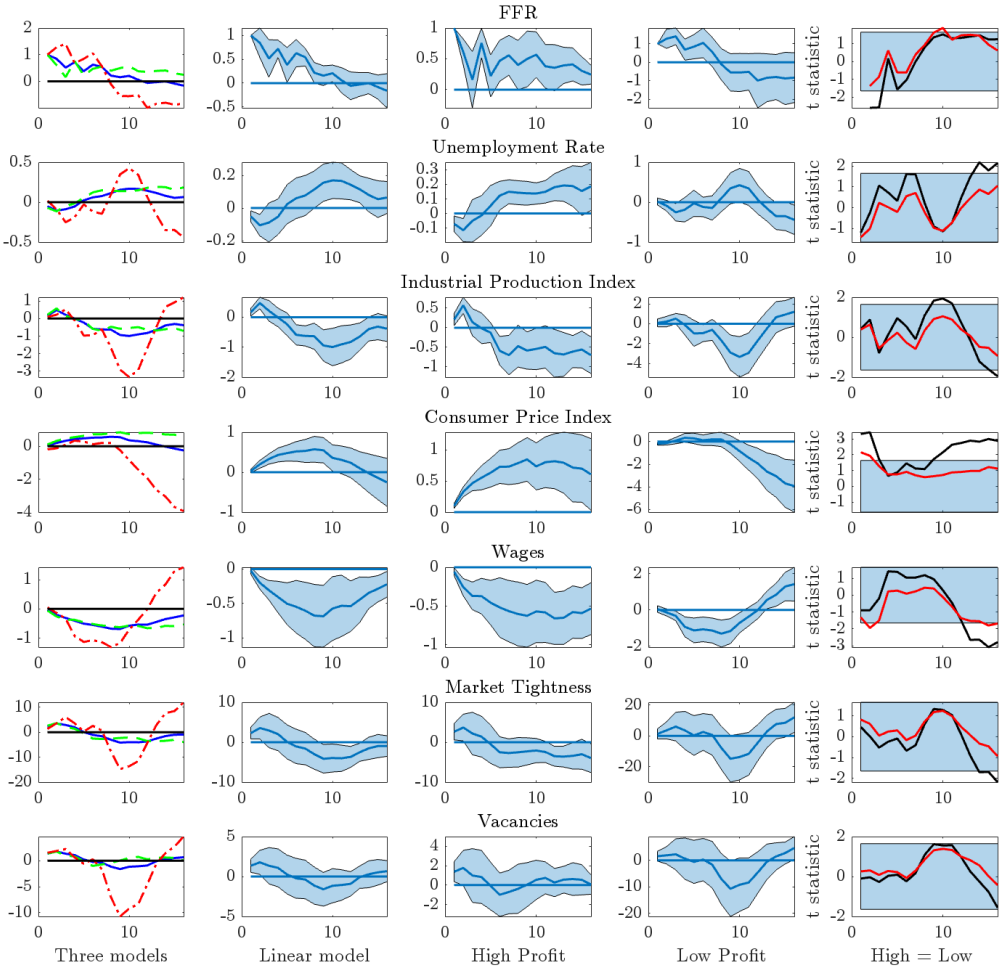


Figure B3: Smooth Transition Local Projections Using Total Factor Productivity as a Proxy for Surplus



Note: The first four columns show the response of the outcome variable to a 1 percentage point change in the FFR on impact across 16 horizons (quarters). In the first column, the average response (solid), the high-surplus (dashed) and the low-surplus (dash-dot) are shown on the same axis. The next three columns show the average response, high-surplus and low-surplus response respectively, with 90% confidence intervals. The last column tests the hypothesis that the coefficients in the high and low surplus regime are equal, where the red line is computed using a Bootstrap, and the black line using the Driscoll-Kraay method, and shaded area is ± 1.65. For details we refer to Tenreyro and Thwaites (2016).

Figure B4: Smooth Transition Local Projections Using Profit as a Proxy for Surplus



Note: The first four columns show the response of the outcome variable to a 1 percentage point change in the FFR on impact across 16 horizons (quarters). In the first column, the average response (solid), the high-surplus (dashed) and the low-surplus (dash-dot) are shown on the same axis. The next three columns show the average response, high-surplus and low-surplus response respectively, with 90% confidence intervals. The last column tests the hypothesis that the coefficients in the high and low surplus regime are equal, where the red line is computed using a Bootstrap, and the black line using the Driscoll-Kraay method, and shaded area is ± 1.65. For details we refer to Tenreyro and Thwaites (2016).

C Comparison to Tenreyro and Thwaites (2016)

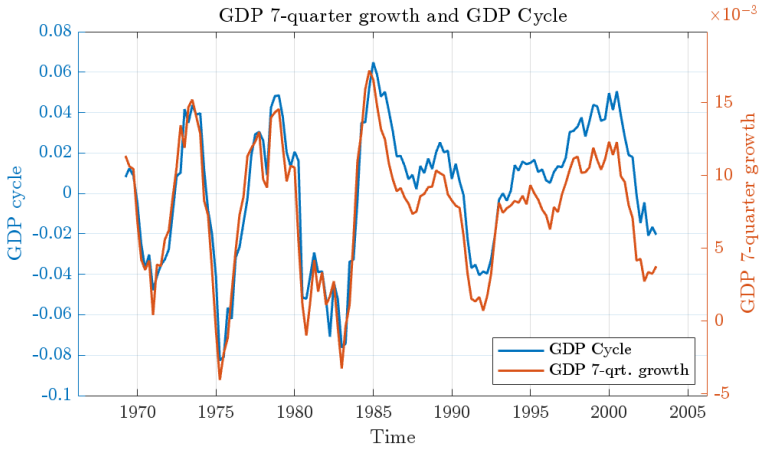
Tenreyro and Thwaites (2016) find that monetary policy has larger effects during expansions than during recessions. At first glance, this may seem to contradict our findings, as one may think that expansions are high surplus periods, and our results instead suggest that monetary policy has smaller real-side effects when surplus is high.

To understand how our results can co-exist with those of Tenreyro and Thwaites (2016), one has to revisit the definition of expansions and recessions in Tenreyro and Thwaites (2016). In particular, their state variable is defined as a seven-quarter moving average of GDP growth. We show in Figure C1 that this seven-quarter moving average roughly coincides with the cycle-component of the Hamilton filter of GDP, hence we believe their state indicator is best interpreted as an indicator of whether GDP is above or below trend.

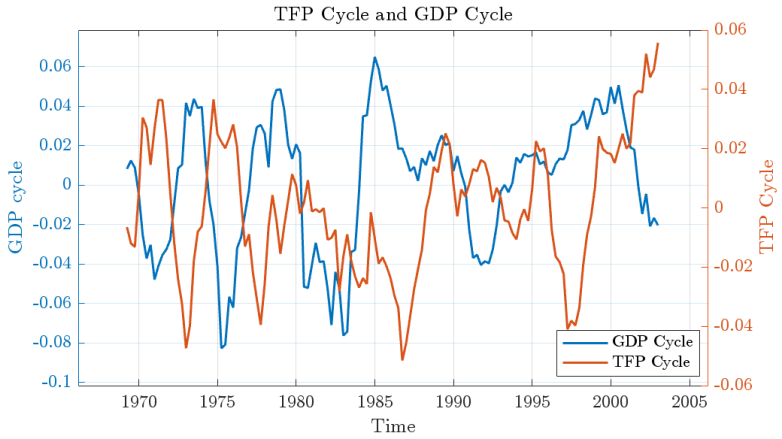
Furthermore, we show in Figure C1 that our surplus proxies are negatively correlated with this state variable. For example, our indicator for TFP tends to be low when GDP is above trend, as is the marginal cost of hiring. This is intuitively, given that when a variable is above trend, it is at its peak, which is when the marginal hiring costs are high and the economy is about to start slowing down. This explains why we find evidence that the effect of monetary policy shocks is larger during times of low surplus, which coincides with periods in time when GDP is above trend.

Figure C1: Time Series over the Tenreyro and Thwaites (2016) Sample.

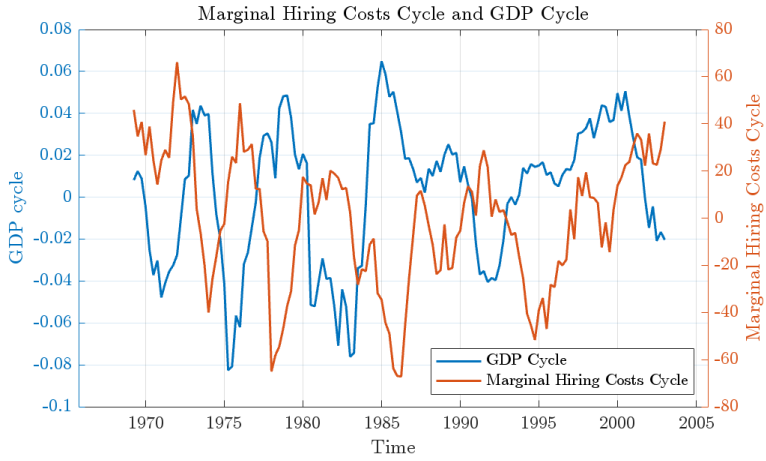
(a) GDP Cycle (Hamilton Filter) and 7-quarter Average of GDP growth.



(b) GDP Cycle (Hamilton Filter) and TFP (Cycle).



(c) GDP Cycle (Hamilton Filter) and Marginal Hiring Cost (Cycle).



D Analytical log-linearization

D.1 Smaller version of the model

We first consider the small NKDMP model of Section 5.2.

Equilibrium Conditions

$$1 = \beta E_t \left[\frac{R_t}{\Pi_{t+1}} \left(\frac{C_{t+1}}{C_t} \right)^{-\tau} \right] \tag{D.1}$$

$$\frac{\omega_t}{\gamma} - 1 = -\phi(\Pi_t - \Pi)\Pi_t + \phi \mathbb{E}_t \left[Q_{t,t+1}(\Pi_{t+1} - \Pi)\Pi_{t+1} \frac{Y_{t+1}}{Y_t} \right] \tag{D.2}$$

$$C_t = Y_t = Z_t N_t \tag{D.3}$$

$$N_t = (1-\delta)N_{t-1} + q_t V_t \tag{D.4}$$

$$\ln Z_{t+1} = \rho_z \ln Z_t + \epsilon_{z,t+1} \tag{D.5}$$

$$q_t = \chi \left(1 + \theta_t^{\iota}\right)^{\frac{-1}{\iota}} \tag{D.6}$$

$$\theta_t = \frac{V_t + X_t}{1 - (1-\delta)N_{t-1}} \tag{D.7}$$

$$\frac{\kappa}{q_t} = (1-\omega_t)Z_t - w_t + (1-\delta)E_t \left[Q_{t,t+1} \frac{\kappa}{q_{t+1}} \right] \tag{D.8}$$

$$w_t = \eta(1-\omega_t)Z_t + (1-\eta)\nu + \eta(1-\delta)\kappa E_t \left[Q_{t,t+1}\theta_{t+1} \right] \tag{D.9}$$

$$\frac{R_t}{\bar{R}} = \left[\left(\frac{\Pi_t}{\bar{\Pi}} \right)^{\psi_1} \left(\frac{Y_t}{\bar{Y}} \right)^{\psi_2} \right]^{1-\rho_R} \left(\frac{R_{t-1}}{\bar{R}} \right)^{\rho_R} e^{\epsilon_{R,t}} \tag{D.10}$$

Steady State We consider a steady state with $\Pi = 1$.

$$\pi = 1 \tag{D.11}$$
$$R = \beta^{-1} \tag{D.12}$$
$$\omega = \gamma \tag{D.13}$$
$$Z = 1 \tag{D.14}$$
$$C = Y = N \tag{D.15}$$
$$\delta N = qV \tag{D.16}$$
$$\theta = \frac{V}{1-(1-\delta)N} \tag{D.17}$$
$$q(\theta) = \chi\left(1+\theta^{\iota}\right)^{\frac{-1}{\iota}} \tag{D.18}$$
$$w = \eta\left[1-\gamma+(1-\delta)\beta\kappa\theta\right]+(1-\eta)\nu \tag{D.19}$$
$$w = 1-\gamma-\frac{\kappa}{q(\theta)}\left[1-(1-\delta)\beta\right] \tag{D.20}$$

Log-Linear Solution

$$E_t\left[\hat{y}_{t+1}\right] = \hat{y}_t + \frac{1}{\tau}E_t\left[\hat{r}_t - \hat{\pi}_{t+1}\right] \tag{D.21}$$
$$\hat{c}_t = \hat{y}_t = \hat{z}_t + \hat{n}_t \tag{D.22}$$
$$\hat{n}_t = (1-\delta)\hat{n}_{t-1} + \delta\left(\hat{q}_t + \hat{v}_t\right) \tag{D.23}$$
$$\hat{z}_t = \rho_z\hat{z}_{t-1} + \epsilon_{z,t} \tag{D.24}$$
$$\hat{r}_t = (1-\rho_R)\left[\psi_1\hat{\pi}_t + \psi_2\hat{y}_t\right] + \rho_R\hat{r}_{t-1} + \epsilon_{R,t} \tag{D.25}$$
$$\hat{\pi}_t = \beta E_t\left[\hat{\pi}_{t+1}\right] - \frac{1}{\phi}\hat{\omega}_t \tag{D.26}$$
$$\hat{w}_t = \frac{(1-\gamma)\hat{z}_t - \gamma\hat{\omega}_t + (1-\delta)\kappa\beta\theta E_t\left[\hat{\pi}_{t+1} - \hat{r}_t + \hat{\theta}_{t+1}\right]}{1-\gamma+\frac{1-\eta}{\eta}\nu + (1-\delta)\kappa\beta\theta} \tag{D.27}$$
$$\hat{q}_t = \frac{-1}{1+\theta^{\iota}}\hat{\theta}_t \tag{D.28}$$
$$\hat{\theta}_t = \hat{v}_t + \frac{(1-\delta)N}{1-(1-\delta)N}\hat{n}_{t-1} \tag{D.29}$$
$$\begin{aligned}\hat{q}_t = {} & \frac{\gamma(1-\beta(1-\delta))}{1-\gamma-w}\hat{\omega}_t + \frac{(\gamma-1)(1-\beta(1-\delta))}{1-\gamma-w}\hat{z}_t + \frac{w(1-\beta(1-\delta))}{1-\gamma-w}\hat{w}_t \ldots \\ & + (1-\delta)\beta E_t[\hat{q}_{t+1} + \hat{r}_t - \hat{\pi}_{t+1}]\end{aligned} \tag{D.30}$$

These ten equations determine the dynamics of the ten variables $\left\{\hat{y}_t, \hat{r}_t, \hat{\pi}_t, \hat{z}_t, \hat{n}_t, \hat{q}_t, \hat{v}_t, \hat{w}_t, \hat{\omega}_t, \hat{\theta}_t\right\}$.

D.2 Quantitative Model Equilibrium

The first-order condition for bonds leads to the following Euler equation

$$1 = \beta \mathbb{E}_t \left[\left(\frac{\lambda_{t+1}}{\lambda_t} \right)^{-\tau} \frac{R_t}{\Pi_{t+1}} \right].$$

Optimal price setting and vacancy posting gives the following pricing equation

$$\frac{\omega_t}{\gamma} = 1 - \phi(\Pi_t - \bar{\Pi})\Pi_t + \phi\beta \mathbb{E}_t \left[\left(\frac{\lambda_{t+1}}{\lambda_t} \right)^{-\tau} \left(\frac{Y_{t+1}}{Y_t} \right) (\Pi_{t+1} - \bar{\Pi})\Pi_{t+1} \right].$$

The expression for the Nash wage and optimal vacancy posting decision by firms leads to the following job-creation condition

$$\frac{\kappa}{q_t} = (1-\eta)\left[(1-\omega_t)Z_t - \nu\right] + \beta(1-\delta)\mathbb{E}_t \left[\left(\frac{\lambda_{t+1}}{\lambda_t} \right)^{-\tau} \frac{\kappa}{q_{t+1}} \right]$$

To close the model, the interest rate rule and law of motion for employment are given by

$$\begin{aligned}
R_t &= \zeta \log\left(e^{1/\zeta} + e^{\tilde{R}_t e^{m_t}/\zeta} \right) \\
\tilde{R}_t &= R \left(\frac{\Pi_t}{\bar{\Pi}} \right)^{\psi_\pi} \left(\frac{Y_t}{Y_{t-1}} \right)^{\psi_y} \\
N_t &= (1-\delta)N_{t-1} + \underbrace{q_t \theta_t \left[1 - (1-\delta)N_{t-1}\right]}_{= q_t V_t}
\end{aligned}$$

A minimum state variable representation of the model has five states $\mathbb{S}_t = \{N_{t-1}, Z_t, m_t, Z_{t-1}, D_t\}$ and three policies $\{\Pi(\mathbb{S}_t), \omega(\mathbb{S}_t), \theta(\mathbb{S}_t)\}$.

E Textbook New-Keynesian Model

E.1 Households

There is a representative infinitely lived household that maximizes

$$\mathbb{E}_0 \left[\sum_{t=0}^{\infty} \beta^t D_t U\left(C_t, N_t\right) \right]$$

subject to a sequence of budget constraints

$$P_t C_t + B_t = R_{t-1} B_{t-1} + P_t W_t N_t + T_t$$

where C_t is consumption of the final good, B_t is an uncontingent nominal bond, R_{t-1} is the nominal interest rate, W_t is the real wage, and T_t contains dividends from firms net of taxes and transfers from the government. We assume utility has the following form

$$U\left(C_t, N_t\right) = \begin{cases} \frac{C_t^{1-\tau}-1}{1-\tau} - \chi \frac{N_t^{1+\eta}}{1+\eta}, \text{ if } \tau \neq 1 \\ \log(C_t) - \chi \frac{N_t^{1+\eta}}{1+\eta}, \text{ if } \tau = 1 \end{cases}$$

where $d_t = \log(D_t)$ is a random shock to the utility of consumption and follows an AR(1)

$$d_{t+1} = \rho_d d_t + \varepsilon_t^d, \quad \varepsilon_t^d \sim N(0, \sigma_d^2)$$

The optimal consumptions/saving and labor supply decisions are given by

$$\begin{aligned} \frac{\chi N_t^{\eta}}{C_t^{-\tau}} &= W_t \\ 1 &= \beta \mathbb{E}_t \left[\frac{D_{t+1}}{D_t} \left(\frac{C_{t+1}}{C_t} \right)^{-\tau} \frac{R_t}{\Pi_{t+1}} \right] \end{aligned}$$

where $\Pi_{t+1} = \frac{P_{t+1}}{P_t}$. The stochastic discount factor is defined as

$$Q_{t,t+1} = \beta \frac{D_{t+1}}{D_t} \left(\frac{C_{t+1}}{C_t} \right)^{-\tau}$$

E.2 Firms

Perfectly competitive final good firm combine a continuum of intermediate goods $j \in [0, 1]$.

Intermediate good j produced by a monopolist with technology $Y_t(j) = Z_t N_t(j)$ where Z_t is an aggregate technology process common to all firms. These firms choose prices $P_t(j)$ and labor inputs $N_t(j)$ to maximize the present discounted value of profit

$$\mathbb{E}_0 \left[Q_{0,t} \left\{ \frac{P_t(j)}{P_t} Z_t N_t(j) - W_t N_t(j) - \frac{\phi}{2} \left(\frac{P_t(j)}{P_{t-1}(j)} - \Pi \right)^2 Y_t \right\} \right]$$

subject to a sequence of constraints

$$Z_t N_t(j) = \left(\frac{P_t(j)}{P_t} \right)^{-1/\gamma} Y_t$$

Optimal choices of $N_t(j)$ and $P_t(j)$ lead to the following condition

$$\begin{aligned} 0 = & \frac{Z_t N_t(j)}{P_t} - \phi \left(\frac{P_t(j)}{P_{t-1}(j)} - \Pi \right) \frac{Y_t}{P_{t-1,j}} - \frac{1}{\gamma} \left(\frac{P_t(j)}{P_t} - \frac{W_t}{Z_t} \right) \left(\frac{P_t(j)}{P_t} \right)^{-1/\gamma - 1} \frac{Y_t}{P_t} \\ & + \phi \mathbb{E}_t \left[Q_{t,t+1} \left(\frac{P_{t+1}(j)}{P_t(j)} - \Pi \right) \frac{P_{t+1}(j)}{P_t(j)^2} Y_{t+1} \right] \end{aligned}$$

In a symmetric equilibrium $P_t(j) = P_t$ and $Y_t = Z_t N_t(j)$ for all j so this simplifies to

$$\frac{1}{\gamma} \left(1 - \frac{W_t}{Z_t} \right) = 1 - \phi \left(\Pi_t - \Pi \right) \Pi_t + \phi \mathbb{E}_t \left[Q_{t,t+1} \left(\Pi_{t+1} - \Pi \right) \Pi_{t+1} \frac{Y_{t+1}}{Y_t} \right]$$

E.3 Government

The government levies lump-sum taxes and runs a balanced budget. The monetary authority follows a Taylor type rule

$$\frac{R_t}{R} = \left(\frac{\Pi_t}{\Pi} \right)^{\phi_\pi} \left(\frac{Y_t}{Y} \right)^{\phi_y} e^{m_t}$$

where m_t is an exogenous monetary policy shock that follows an AR(1)

$$m_{t+1} = \rho_m m_t + \varepsilon_t^m, \quad \varepsilon_t^m \sim N(0, \sigma_m^2)$$

E.4 Steady State

We focus on a non-stochastic steady state with inflation π equal to the Central Bank target which implies $R = \Pi/\beta$, and the parameter χ normalizes steady state output Y (that is N) to be unity $\chi = 1 - \gamma$. Note this implies $W = \chi$ so γ is the steady state wage markdown.

E.5 Equilibrium

The equilibrium conditions for market clearing in the labor and goods markets are

$$\begin{aligned} Y_t &= C_t = N_t Z_t \\ W_t &= (1-\gamma) N_t^{\eta} C_t^{\tau} = (1-\gamma) N_t^{\eta+\tau} Z_t^{\tau} \end{aligned}$$

A minimal state representation consists of states $\mathbb{S} = \{z_t, d_t, m_t\}$ and policies $\{\Pi(\mathbb{S}), N(\mathbb{S})\}$ defined through the equilibrium conditions (substituting market clearing conditions where appropriate)

$$\begin{aligned} \text{Euler/IS}: \; 1 &= \beta \mathbb{E}_t \left[e^{(\rho_d - 1) d_t + \epsilon^d_{t+1}} \left(\frac{N_{t+1}}{N_t} e^{(\rho_z - 1) z_t + \epsilon^z_{t+1}} \right)^{-\tau} \frac{R_t}{\Pi_{t+1}} \right] \\ \text{Pricing/NK-Phillips}: \; \frac{1}{\gamma} \left(1 - \chi N_t^{\eta+\tau} e^{(\tau-1) z_t} \right) &= 1 - \phi \left(\Pi_t - \Pi \right) \Pi_t \\ &\quad + \phi \beta \mathbb{E}_t \left[e^{(\rho_d - 1) d_t + \epsilon^d_{t+1}} \left(\frac{N_{t+1}}{N_t} e^{(\rho_z - 1) z_t + \epsilon^z_{t+1}} \right)^{1-\tau} \left(\Pi_{t+1} - \Pi \right) \Pi_{t+1} \right] \end{aligned}$$

and an auxiliary equation

$$\text{Taylor Rule}: \; \frac{R_t}{R} = \left(\frac{\Pi_t}{\Pi} \right)^{\phi_\pi} \left(\frac{N_t Z_t}{Y} \right)^{\phi_y} e^{m_t}$$

Using the steady state relations and letting lower case letters denote log-deviations from steady state values $x = \ln X_t - \ln X$, the equilibrium conditions become

$$\begin{aligned} 1 &= \mathbb{E}_t \left[e^{(\rho_d - 1) d_t + \varepsilon^d_{t+1} - \tau \left(n_{t+1} - n_t + (\rho_z - 1) z_t + \epsilon^z_{t+1} \right) + r_t - \pi_{t+1}} \right] \\ \kappa \left(1 - e^{(\eta+\tau) n_t + (\tau - 1) z} \right) &= - \left(e^{\pi_t} - 1 \right) e^{\pi_t} + \beta \mathbb{E}_t \left[e^{(\rho_d - 1) d_t + \epsilon^d_{t+1} + (1-\tau) \left(n_{t+1} - n_t + (\rho_z - 1) z_t + \varepsilon^z_{t+1} \right)} \left(e^{\pi_{t+1}} - 1 \right) e^{\pi_{t+1}} \right] \\ r_t &= \phi_\pi \pi_t + \phi_y (n_t + z + t) + m_t \end{aligned}$$

where $\kappa = \frac{1-\gamma}{\phi \Pi^2 \gamma}$

E.6 Log-linear System

Lowercase signifies log-deviation from steady state

$$
\begin{aligned}
n_t &= \mathbb{E}_t[n_{t+1}] + \frac{1}{\tau}(1-\rho_d)d_t - (1-\rho_z)z_t - \frac{1}{\tau}\left\{r_t - \mathbb{E}_t[\pi_{t+1}]\right\} \\
\pi_t &= \beta\mathbb{E}_t[\pi_{t+1}] + \kappa\left[(\eta+\tau)n_t + (\tau-1)z_t\right] \\
r_t &= \phi_\pi\pi_t + \phi_y(n_t+z_t) + m_t \\
m_t &= \rho_m m_{t-1} + \varepsilon_t^m \\
z_t &= \rho_z z_{t-1} + \varepsilon_t^z \\
d_t &= \rho_d d_{t-1} + \varepsilon_t^d
\end{aligned}
$$

E.7 Local Approximation

Note, we can write the variables of the equilibrium system in terms of log deviations from steady state (lowercase signifies logs, e.g, $\pi_t = \ln\Pi_t - \ln\Pi$), after substituting the Taylor Rule into the Euler equation, as

$$
\begin{aligned}
1 =& \mathbb{E}_t\left[e^{(\rho_d-1)d_t+\epsilon^d_{t+1}-\tau\left\{n_{t+1}-n_t+(\rho_z-1)z_t+\epsilon^z_{t+1}\right\}+\phi_\pi\pi_t+\phi_y(n_t+z_t)+m_t-\pi_{t+1}}\right] \\
\frac{1-\gamma}{\Pi^2\phi\gamma}\left(1-e^{(\eta+\tau)n_t+(\tau-1)z_t}\right) =& -\left(e^{\pi_t}-1\right)e^{\pi_t} \\
&+\beta\mathbb{E}_t\left[e^{(\rho_d-1)d_t+\epsilon^d_{t+1}+(1-\tau)\left\{n_{t+1}-n_t+(\rho_z-1)z_t+\epsilon^z_{t+1}\right\}}\left(e^{\pi_{t+1}}-1\right)e^{\pi_{t+1}}\right]
\end{aligned}
$$

Which can be simplified to

$$
\begin{aligned}
1 =& e^{(\rho_d-1)d_t+\tau n_t+\tau(1-\rho_z)z_t+\phi_\pi\pi_t+\phi_y(n_t+z_t)+m_t}\mathbb{E}_t\left[e^{\epsilon^d_{t+1}-\tau n_{t+1}-\tau\epsilon^z_{t+1}-\pi_{t+1}}\right] \\
\frac{1-\gamma}{\Pi^2\phi\gamma}\left(1-e^{(\eta+\tau)n_t+(\tau-1)z_t}\right) =& -e^{2\pi_t}+e^{\pi_t} \\
&+\beta\mathbb{E}_t\left[e^{(\rho_d-1)d_t+\epsilon^d_{t+1}+(1-\tau)\left\{n_{t+1}-n_t+(\rho_z-1)z_t+\epsilon^z_{t+1}\right\}+2\pi_{t+1}}\right] \\
&-\beta\mathbb{E}_t\left[e^{(\rho_d-1)d_t+\epsilon^d_{t+1}+(1-\tau)\left\{n_{t+1}-n_t+(\rho_z-1)z_t+\epsilon^z_{t+1}\right\}+\pi_{t+1}}\right]
\end{aligned}
$$

The first step is to suppose the policies are linear in logs

$$
\begin{aligned}
\pi_t &= a_0 + a_1 z_t + a_2 d_t + a_3 m_t \\
n_t &= b_0 + b_1 z_t + b_2 d_t + b_3 m_t
\end{aligned}
$$

This implies the future policies are of the form

$$\pi_{t+1} = a_0 + a_1\rho_z z_t + a_1\epsilon^z_{t+1} + a_2\rho_d d_t + a_2\epsilon^d_{t+1} + a_3\rho_m m_t + a_3\epsilon^m_{t+1}$$
$$n_{t+1} = b_0 + b_1\rho_z z_t + b_1\epsilon^z_{t+1} + b_2\rho_d d_t + b_2\epsilon^d_{t+1} + b_3\rho_m m_t + b_3\epsilon^m_{t+1}$$

Moreover, it implies

$$n_{t+1} - n_t = b_1(\rho_z - 1)z_t + b_1\epsilon^z_{t+1} + b_2(\rho_d - 1)d_t + b_2\epsilon^d_{t+1} + b_3(\rho_m - 1)m_t + b_3\epsilon^m_{t+1}$$

The goal of the local approximation method is to solve for the policy coefficients $\boldsymbol{a}$ and $\boldsymbol{b}$ as implicit functions of the current state (z_t, d_t, m_t).

Euler equation. Consider the Euler equation with the policies substituted

$$\begin{aligned} 1 =& e^{(\rho_d-1)d_t - \tau[b_1(\rho_z-1)z_t + b_2(\rho_d-1)d_t + b_3(\rho_m-1)m_t] - \tau(\rho_z-1)z_t + r_t - a_1 - a_1\rho_z z_t - a_2\rho_d d_t - a_3\rho_m m_t} \\ & \cdot \mathbb{E}_t\left[e^{\epsilon^d_{t+1} - \tau(b_1\epsilon^z_{t+1} + b_2\epsilon^d_{t+1} + b_3\epsilon^m_{t+1}) - \tau\epsilon^z_{t+1} - a_1\epsilon^z_{t+1} - a_2\epsilon^d_{t+1} - a_3\epsilon^m_{t+1}}\right] \end{aligned}$$

Collecting terms in the expectation yields

$$\mathbb{E}_t\left[e^{\epsilon^d_{t+1} - \tau(b_1\epsilon^z_{t+1} + b_2\epsilon^d_{t+1} + b_3\epsilon^m_{t+1}) - \tau\epsilon^z_{t+1} - a_1\epsilon^z_{t+1} - a_2\epsilon^d_{t+1} - a_3\epsilon^m_{t+1}}\right] = \mathbb{E}_t\left[e^{(1-\tau b_2 - a_2)\epsilon^d_{t+1} - (\tau(b_1+1)+a_1)\epsilon^z_{t+1} - \tau(b_3+a_3)\epsilon^m_{t+1}}\right]$$

For a mean zero normal random variable X, and constant c, the expectation satisfies

$$\mathbb{E}\left[e^{cX}\right] = e^{\frac{1}{2}c^2\sigma_x^2},$$

so the Euler equation simplifies to

$$\begin{aligned} 1 =& e^{(\rho_d-1)d_t - \tau[b_1(\rho_z-1)z_t + b_2(\rho_d-1)d_t + b_3(\rho_m-1)m_t] - \tau(\rho_z-1)z_t + r_t - a_1 - a_1\rho_z z_t - a_2\rho_d d_t - a_3\rho_m m_t} \\ & \cdot e^{\frac{1}{2}\left\{(1-\tau b_2 - a_2)^2\sigma_d^2 + (\tau(b_1+1)+a_1)^2\sigma_z^2 + \tau^2(b_3+a_3)^2\sigma_m^2\right\}} \end{aligned}$$

Note, by taking logs and substituting the Taylor Rule, this is equivalent to

$$
\begin{aligned}
0 = &(\rho_d - 1)d_t + \tau\left[b_1(1-\rho_z)z_t + b_2(1-\rho_d)d_t + b_3(1-\rho_m)m_t\right] + \tau(1-\rho_z)z_t \\
&+ \phi_\pi(a_0 + a_1 z_t + a_2 d_t + a_3 m_t) + \phi_y(b_0 + b_1 z_t + b_2 d_t + b_3 m_t + z_t) + m_t \\
&- (a_0 + a_1\rho_z z_t + a_2\rho_d d_t + a_3\rho_m m_t) \\
&+ \frac{1}{2}\left\{(1-\tau b_2 - a_2)^2\sigma_d^2 + (\tau(b_1+1)+a_1)^2\sigma_z^2 + \tau^2(b_3+a_3)^2\sigma_m^2\right\}
\end{aligned}
$$

which implies the variance terms show up in the Euler equation, but not the partial derivatives of the Euler equation with respect to the states. The partial derivatives w.r.t. the policy coefficients are given by

$$
\begin{aligned}
&\partial b_0 : \phi_y \\
&\partial b_1 : \left[\tau(1-\rho_z) + \phi_y\right] z_t + \tau\left(\tau(b_1+1)+a_1\right)\sigma_z^2 \\
&\partial b_2 : \left[\tau(1-\rho_d) + \phi_y\right] d_t - \tau\left(1-\tau b_2 - a_2\right)\sigma_d^2 \\
&\partial b_3 : \left[\tau(1-\rho_m) + \phi_y\right] m_t + \tau^2\left(b_3 + a_3\right)\sigma_m^2 \\
&\partial a_0 : \phi_p - 1 \\
&\partial a_1 : (\phi_p - \rho_z) z_t + \left(\tau(b_1+1)+a_1\right)\sigma_z^2 \\
&\partial a_2 : (\phi_p - \rho_d) d_t - \left(1-\tau b_2 - a_2\right)\sigma_d^2 \\
&\partial a_3 : (\phi_p - \rho_m) m_t + \tau^2\left(b_3 + a_3\right)\sigma_m^2
\end{aligned}
$$

Moreover, the partial derivatives with respect to the states are given by

$$
\begin{aligned}
\partial z_t &: 0 = \tau b_1 + \tau(1-\rho_z) + \phi_\pi a_1 + \phi_y b_1 - \tau b_1\rho_z - a_1\rho_z \\
&\Rightarrow 0 = \tau(1-\rho_z) + \left[\tau(1-\rho_z) + \phi_y\right] b_1 + (\phi_\pi - \rho_z) a_1 \\
\partial z_t \partial b_1 &: \tau(1-\rho_z) + \phi_y \\
\partial z_t \partial a_1 &: \phi_\pi - \rho_z
\end{aligned}
$$

$$
\begin{aligned}
\partial d_t &: 0 = (\rho_d - 1) + \tau b_2 + \phi_\pi a_2 + \phi_y b_2 - \tau b_2\rho_d - a_2\rho_d \\
&\Rightarrow 0 = (\rho_d - 1) + \left[\tau(1-\rho_d) + \phi_y\right] b_2 + (\phi_\pi - \rho_d) a_2 \\
\partial d_t \partial b_2 &: \tau(1-\rho_d) + \phi_y \\
\partial d_t \partial a_2 &: \phi_\pi - \rho_d
\end{aligned}
$$

$$
\begin{aligned}
\partial m_t : 0 &= \tau b_3 + \phi_\pi a_3 + \phi_y b_3 + 1 - \tau b_3 \rho_m - a_3 \rho_m \\
\Rightarrow 0 &= 1 + \left[\tau(1-\rho_m) + \phi_y\right] b_3 + (\phi_\pi - \rho_m) a_3 \\
\partial m_t \partial b_3 &: \tau(1-\rho_m) + \phi_y \\
\partial m_t \partial a_3 &: \phi_\pi - \rho_m
\end{aligned}
$$

which gives the residual function derivatives and elements of the Jacobian related to the Euler equation. Note, only the elements of the Jacobian that depend on the policy coefficients $\boldsymbol{a}$ and $\boldsymbol{b}$ need to be updated in the Newton solution step. Of the 64 elements of the Jacobian, 32 are determined by the Euler equation block, of which *only* 6 depend on the policy coefficients.

Pricing equation. Now consider the pricing equation with the policies substituted

$$
\begin{aligned}
&\frac{1-\gamma}{\Pi^2 \phi \gamma}\left(1 - e^{(\eta+\tau)(b_0+b_1 z_t+b_2 d_t+b_3 m_t)+(\tau-1)z_t}\right) = -e^{2(a_0+a_1 z_t+a_2 d_t+a_3 m_t)} + e^{a_0+a_1 z_t+a_2 d_t+a_3 m_t} \\
&+ \beta e^{(\rho_d-1)d_t+(1-\tau)\{b_1(\rho_z-1)z_t+b_2(\rho_d-1)d_t+b_3(\rho_m-1)m_t+(\rho_z-1)z_t\}+2(a_0+a_1\rho_z z_t+a_2\rho_d d_t+a_3\rho_m m_t)} \\
&\cdot \mathbb{E}_t\left[e^{\epsilon^d_{t+1}+(1-\tau)\left\{b_1\epsilon^z_{t+1}+b_2\epsilon^d_{t+1}+b_3\epsilon^m_{t+1}+\epsilon^z_{t+1}\right\}+2(a_1\epsilon^z_{t+1}+a_2\epsilon^d_{t+1}+a_3\epsilon^m_{t+1})}\right] \\
&- \beta e^{(\rho_d-1)d_t+(1-\tau)\{b_1(\rho_z-1)z_t+b_2(\rho_d-1)d_t+b_3(\rho_m-1)m_t+(\rho_z-1)z_t\}+a_0+a_1\rho_z z_t+a_2\rho_d d_t+a_3\rho_m m_t} \\
&\cdot \mathbb{E}_t\left[e^{\epsilon^d_{t+1}+(1-\tau)\left\{b_1\epsilon^z_{t+1}+b_2\epsilon^d_{t+1}+b_3\epsilon^m_{t+1}+\epsilon^z_{t+1}\right\}+a_1\epsilon^z_{t+1}+a_2\epsilon^d_{t+1}+a_3\epsilon^m_{t+1}}\right]
\end{aligned}
$$

focusing on the expectation terms, we have the following

$$
\begin{aligned}
&\mathbb{E}_t\left[e^{\epsilon^d_{t+1}+(1-\tau)\left\{b_1\epsilon^z_{t+1}+b_2\epsilon^d_{t+1}+b_3\epsilon^m_{t+1}+\epsilon^z_{t+1}\right\}+2(a_1\epsilon^z_{t+1}+a_2\epsilon^d_{t+1}+a_3\epsilon^m_{t+1})}\right] \\
&= \mathbb{E}_t\left[e^{(1+(1-\tau)b_2+2a_2)\epsilon^d_{t+1}+((1-\tau)(b_1+1)+2a_1)\epsilon^z_{t+1}+((1-\tau)b_3+2a_3)\epsilon^m_{t+1}}\right] \\
&= e^{\frac{1}{2}\left\{(1+(1-\tau)b_2+2a_2)^2\sigma_d^2+((1-\tau)(b_1+1)+2a_1)^2\sigma_z^2+((1-\tau)b_3+2a_3)^2\sigma_m^2\right\}}
\end{aligned}
$$

$$
\begin{aligned}
&\mathbb{E}_t\left[e^{\epsilon^d_{t+1}+(1-\tau)\left\{b_1\epsilon^z_{t+1}+b_2\epsilon^d_{t+1}+b_3\epsilon^m_{t+1}+\epsilon^z_{t+1}\right\}+a_1\epsilon^z_{t+1}+a_2\epsilon^d_{t+1}+a_3\epsilon^m_{t+1}}\right] \\
&= \mathbb{E}_t\left[e^{(1+(1-\tau)b_2+a_2)\epsilon^d_{t+1}+((1-\tau)(b_1+1)+a_1)\epsilon^z_{t+1}+((1-\tau)b_3+a_3)\epsilon^m_{t+1}}\right] \\
&= e^{\frac{1}{2}\left\{(1+(1-\tau)b_2+a_2)^2\sigma_d^2+((1-\tau)(b_1+1)+a_1)^2\sigma_z^2+((1-\tau)b_3+a_3)^2\sigma_m^2\right\}}
\end{aligned}
$$

which implies the pricing equation simplifies to

$$\kappa\left(1-e^{(\eta+\tau)(b_0+b_1z_t+b_2d_t+b_3m_t)+(\tau-1)z_t}\right)=-e^{2(a_0+a_1z_t+a_2d_t+a_3m_t)}+e^{a_0+a_1z_t+a_2d_t+a_3m_t}$$
$$+\beta e^{(\rho_d-1)d_t+(1-\tau)\{b_1(\rho_z-1)z_t+b_2(\rho_d-1)d_t+b_3(\rho_m-1)m_t+(\rho_z-1)z_t\}+2(a_0+a_1\rho_zz_t+a_2\rho_dd_t+a_3\rho_mm_t)}$$
$$\cdot e^{\frac{1}{2}\left\{(1+(1-\tau)b_2+2a_2)^2\sigma_d^2+((1-\tau)(b_1+1)+2a_1)^2\sigma_z^2+((1-\tau)b_3+2a_3)^2\sigma_m^2\right\}}$$
$$-\beta e^{(\rho_d-1)d_t+(1-\tau)\{b_1(\rho_z-1)z_t+b_2(\rho_d-1)d_t+b_3(\rho_m-1)m_t+(\rho_z-1)z_t\}+a_0+a_1\rho_zz_t+a_2\rho_dd_t+a_3\rho_mm_t}$$
$$\cdot e^{\frac{1}{2}\left\{(1+(1-\tau)b_2+a_2)^2\sigma_d^2+((1-\tau)(b_1+1)+a_1)^2\sigma_z^2+((1-\tau)b_3+a_3)^2\sigma_m^2\right\}}$$

where $\kappa=\frac{1-\gamma}{\Pi^2\phi\gamma}$. Here, the derivatives of the residual function and elements of the Jacobian are more elaborate, but given that this is an analytic expression we can rely on symbolic differentiation to obtain the results.